Atmos. Chem. Phys., 24, 13129–13150, 2024
https://doi.org/10.5194/acp-24-13129-2024

Atmospheric Chemistry and Physics
Open Access
EGU

Research article

Reactive chlorine-, sulfur-, and nitrogen-containing volatile organic compounds impact atmospheric chemistry in the megacity of Delhi during both clean and extremely polluted seasons

Sachin Mishra[1], Vinayak Sinha[1], Haseeb Hakkim[1], Arpit Awasthi[1], Sachin D. Ghude[2], Vijay Kumar Soni[3], Narendra Nigam[3], Baerbel Sinha[1], and Madhavan N. Rajeevan[4]

[1]Department of Earth and Environmental Sciences, Indian Institute of Science Education and Research Mohali, Sector 81, S.A.S Nagar, Manauli PO, Punjab 140306, India
[2]Indian Institute of Tropical Meteorology, Ministry of Earth Sciences, Pashan, Pune 411 008, India
[3]India Meteorological Department, Ministry of Earth Sciences, India, New Delhi 110 003, India
[4]Ministry of Earth Sciences, Government of India, New Delhi 110 003, India

Correspondence: Vinayak Sinha (vsinha@iisermohali.ac.in)

Received: 20 February 2024 – Discussion started: 29 February 2024
Revised: 26 September 2024 – Accepted: 30 September 2024 – Published: 28 November 2024

Abstract. Volatile organic compounds (VOCs) significantly impact the atmospheric chemistry of polluted megacities. Delhi is a dynamically changing megacity, and yet our knowledge of its ambient VOC composition and chemistry is limited to few studies conducted mainly in winter before 2020 (all pre-COVID-19). Here, using a new extended volatility range high-mass-resolution (10 000–15 000) proton transfer reaction time-of-flight mass spectrometer, we measured and analysed ambient VOC mass spectra acquired continuously over a 4-month period, covering "clean" monsoon (July–September) and "polluted" post-monsoon seasons, for the year 2022. Out of 1126 peaks, 111 VOC species were identified unambiguously. Averaged total mass concentrations reached $\sim 260\,\mu g\,m^{-3}$ and were > 4 times in the polluted season relative to the cleaner season, as driven by enhanced emissions from biomass burning and reduced atmospheric ventilation (~ 2). Among 111, 56 were oxygenated, 10 contained nitrogen, 2 chlorine, 1 sulfur, and 42 were pure hydrocarbons. VOC levels during polluted periods were significantly higher than most developed world megacities. Methanethiol, dichlorobenzenes, C6 amides, and C9 organic acids/esters, which have previously never been reported in India, were detected in both the clean and polluted periods. The sources were industrial for methanethiol and dichlorobenzenes, purely photochemical for the C6 amides, and multiphase oxidation and partitioning for C9 organic acids. Aromatic VOC / CO emission ratio analyses indicated additional biomass combustion/industrial sources in the post-monsoon season, along with year-round traffic sources in both seasons. Overall, the unprecedented new information concerning ambient VOC speciation, abundance, variability, and emission characteristics during contrasting seasons significantly advances current atmospheric composition understanding of highly polluted urban atmospheric environments like Delhi.

Published by Copernicus Publications on behalf of the European Geosciences Union.

1 Introduction

The national capital territory of Delhi in India is jointly administered by the central and state governments and accommodated more than 32 million people in 2022. For the past several years, its population has grown at the rate of more than 2.7 % yr^{-1}, adding about 1 million new inhabitants each year. Thus, the region represents a complex and dynamically changing emission environment driven by rapid changes in emissions as regulatory authorities make efforts to improve urban infrastructure and public transportation, while promoting cleaner technologies. As a megacity in a developing country with one of the world's highest population densities, Delhi exemplifies some of the key challenges faced by many megacities in the Global South, where increased urbanization and inequitable access to clean-energy sources, along with unfavourable meteorological conditions during cold periods of the year, cause the inhabitants to suffer from extreme air pollution episodes. Lelieveld et al. (2015) identified South Asia as one of the global air pollution hotspots in terms of the contribution of outdoor air pollution sources to premature mortality due to particulate matter pollution. Reduction in other atmospheric pollutants is also deemed necessary to fulfil the UN Sustainable Development Goals (Keywood et al., 2023). Thus, the study of Delhi's ambient chemical composition using state-of-the-art technology can offer valuable insights and lessons for our understanding of polluted atmospheric environments.

Previous studies have demonstrated that air pollution in the Delhi National Capital Region (NCR) metropolitan area peaks during the post-monsoon (October–November) season (e.g. Kulkarni et al., 2020), coinciding with the time of year when large-scale paddy stubble burning occurs in the Indo-Gangetic Plain (Kumar et al., 2021). The main air pollutant in exceedance has long been identified to be particulate matter (e.g. $PM_{2.5}$), and many studies (Gani et al., 2020; Cash et al., 2021; Sharma and Mandal, 2023; Singh et al., 2011) have documented the variability, exceedance, and composition of aerosols. Volatile organic compounds (VOCs) are major precursors of secondary organic aerosol, which is a significant component of $PM_{2.5}$ (30 %–60 % in Delhi; Chen et al., 2022; Nault et al., 2021) and surface ozone over Delhi. In fact, in situ ozone production in Delhi has been reported to be more sensitive to VOCs rather than nitrogen oxides (Nelson et al., 2021). Several VOCs (e.g. benzene, nitromethane, and 1,3-butadiene) are also carcinogenic (WHO, 2010) at high exposure concentrations, and many pose direct health risks (Ho et al., 2006; Espenship et al., 2019; WHO, 2019; Weng et al., 2009; Roberts et al., 2011; Durmusoglu et al., 2010). VOCs can also aid source apportionment studies by acting as source fingerprints and valuable molecular markers of specific emission sources (de Gouw et al., 2017; Holzinger et al., 1999; Warneke et al., 2001; Kumar et al., 2020; Garg et al., 2016; Hakkim et al., 2021; Kumar et al., 2021). In the complex emission environment of cities in the developing world, this can be especially helpful, since the energy usage portfolio is such that biomass burning sources are likely to be as significant as fossil-fuel-based sources (Bikkina et al., 2019) in influencing the air pollutant burden of VOCs, resulting in ambient-air VOC composition that could be quite different from cities like Los Angeles (McDonald et al., 2018).

Existing knowledge about the abundance and diurnal variability in major ambient VOCs, such as methanol, acetone, acetaldehyde, acetonitrile, isoprene, benzene, toluene, xylenes, and trimethyl benzenes in Delhi, is limited to just four previously measured wintertime data sets: December–March of 2016 (Chandra et al., 2018; Hakkim et al., 2019), December–March of 2018 (Wang et al., 2020; Tripathi et al., 2022), a few days in October 2018 (Nelson et al., 2021; Bryant et al., 2023), and one spanning 145 d in 2019 that reported the source apportionment of some VOCs for different seasons (Jain et al., 2022). We note that all these were pre-COVID-19 period data sets and that since these observations many new regulations have been put in place, e.g., for traffic with the introduction of BS-VI (EURO6 equivalent) in 2020 and the Faster Adoption and Manufacturing of (Hybrid &) Electric vehicles (FAME) programme for the promotion of electric vehicles (EVs) and for industries with a ban on the use of petroleum coke (petcoke) in the National Capital Region (NCR) and the crackdown on unregistered industries (Guttikunda et al., 2023). After COVID-19 lockdowns happened in 2020, a new Commission for Air Quality Management (CAQM) in the Delhi National Capital Region and its adjoining areas was set up in November 2020 (https://caqm.nic.in/index.aspx?langid=1, last access: 10 February 2024). Under its mandate, depending on the air quality level, it promulgates immediate graded response action plans (GRAPs; https://caqm.nic.in/index1.aspx?lsid=4168&lev=2&lid=4171&langid=1, last access: 15 February 2024) that instruct civic authorities to shut down or restrict particular emission sources. Furthermore, on 7 August 2020, the Delhi government announced a new Delhi Electric Vehicle (EV) Policy. In order to address the high upfront cost of EVs (ICE vehicles), the Delhi EV Policy provides demand incentives for purchasing electric vehicles. The incentives help bring cost parity for EVs and are in addition to those outlined in the Faster Adoption and Manufacturing of Hybrid and Electric Vehicles (FAME II). In the budget allocation for 2020, the Government of India allocated USD 600 million for clean-air measures through the Ministry of Housing and Urban Affairs (MOHUA) to 46 cities across India. These have been detailed in a report by Arpan Chatterji (Chatterji, 2020). Thus, overall, important changes to the transport emission sector, construction and urban industrial sector, and residential sector were implemented at a policy level after 2020 to reduce air pollution in the Delhi NCR region.

The monsoon season, which precedes the post-monsoon season, lasts from June to September and is characterized by better air quality, aided by favourable meteorological conditions, including a higher ventilation coefficient, negligi-

ble agricultural waste burning, and enhanced wet scavenging (Kumar et al., 2016).

This study addresses some of the above knowledge gaps pertaining to ambient VOCs during the "clean" monsoon season characterized by baseline pollution levels and the polluted "post-monsoon" season characterized by extreme pollution events and large-scale open agricultural biomass waste fires regionally. Employing a new extended volatility range (EVR) high-mass-resolution (10 000–15 000) proton transfer reaction time-of-flight mass spectrometer 10K (PTR-TOF 10000; Ionicon Analytik GmbH), a technology that has never before been deployed in India, we investigated the ambient VOC speciation, abundance, variability, and emission characteristics in the polluted urban environment of Delhi over a 4-month period. This enabled us to discover several low-volatility VOCs, many of which are present in fire emissions (Koss et al., 2018), for the first time in South Asia, as all previous VOC studies have involved either the older PTR-TOF-MS or PTR-QMS instruments that have significantly lower mass resolution and lower detection sensitivity and did not possess the extended volatility range components. We first undertook a comprehensive and rigorous interpretation of the ambient mass spectra over a 4-month period spanning July–November of 2022 in Delhi. This was followed by the identification and quantification of 111 VOCs, many of which have been discovered and reported for the first time from the South Asian atmospheric environment. Each of these compounds was then classified in terms of oxygenated VOCs, pure hydrocarbons, major nitrogen-containing VOCs, chlorine-containing VOCs, and sulfur-containing VOCs, followed by the time series analyses and diurnal profiles of the major VOCs and some new/rarely reported VOCs in both seasons as a function of meteorology and emissions. The atmospheric chemistry implications of some of the newly discovered compounds in this polluted urban environment are discussed. Further, using measured aromatic VOC / CO emission ratios in the monsoon and post-monsoon season, a global comparison with reports from megacities in Europe, North America, and Asia was undertaken for a nuanced understanding of their levels and sources in Delhi relative to megacities across these different continents.

2 Methodology

2.1 Measurement site and meteorological conditions

The measurement site was located within the premises of the India Meteorological Department (IMD), which is situated in central Delhi (Fig. 1). Ambient air was sampled at a height of circa 35 m a.g.l. (above ground level) from the rooftop of the SatMet Building (28.5896° N–77.2210° E) into the instruments which were housed inside a laboratory located on the sixth floor of the same building.

Figure 1a shows the land use/land cover (Sentinel-2 10 m) map of India, with a box marked red highlighting Delhi. The city is bordered on its northern, western, and southern sides by the state of Haryana and to the east by the state of Uttar Pradesh. The star in Fig. 1b shows the measurement site (IMD Delhi) and its surroundings. The major pollution hotspots include places like Ghaziabad (towards the northeast), Bahadurgarh (towards the northwest), Gurgaon (towards the southwest), and Faridabad and Okhla (towards the southeast). Major industrial areas, e.g. the Okhla industrial area, major landfill sites, the international airport, and some major hospitals, are also shown in Fig. 1b.

Meteorological sensors (Campbell Scientific, Inc.) were deployed to measure the wind speed, direction, temperature, relative humidity, and photosynthetic active radiation (PAR sensor PQSI; model no. CS215 for temperature and RH and model no. TE525-L40 for rain). Boundary layer height was taken from the ERA5 reanalyses data set (Hersbach et al., 2023), and the ventilation coefficient was calculated as the product of the measured wind speed and boundary layer height. Atmospheric ventilation or the ventilation coefficient (VC) is a good proxy for the dilution and dispersion of air pollutants near the surface (Hakkim et al., 2019). It is defined as the product of boundary layer height (m) and wind speed ($m\,s^{-1}$). The VC represents the rate at which air within the mixed layer is transported away from a region of interest and provides information about how concentrations of pollutants are modulated through the transport of air over that region. Figure 1c and d show the wind rose plot derived from the in situ 1 min wind speed and wind direction data acquired at the measurement site for the monsoon (July 2022–September 2022) and post-monsoon (October 2022–November 2022) seasons, respectively. The prevalent wind direction changed from an easterly flow in the monsoon season to a westerly flow in the post-monsoon season. During the monsoon season, the major fetch region spanned from the NE to SE–E. These NE, E, and SE winds were associated with high wind speeds ranging from 3–6 $m\,s^{-1}$, which on occasion reached up to 9 $m\,s^{-1}$. During the post-monsoon season, the major wind flow was from the NW to the SW–W sector. These wind speeds were lower, ranging from 1–3 $m\,s^{-1}$, and they exceeded 6 $m\,s^{-1}$ only occasionally. Overall, the site received air from all wind sectors in both seasons. This is also borne by the back-trajectory analyses presented in the companion paper (Awasthi et al., 2024), which showed that the site is characterized by regional airflow patterns, as documented at other sites in the Indo-Gangetic Plain (Pawar et al., 2015).

Fire count data were obtained using the Visible Infrared Imaging Radiometer Suite (VIIRS) 375 m thermal anomalies/active fire product data from the VIIRS sensor aboard the joint NASA/NOAA Suomi National Polar-orbiting Partnership (Suomi NPP) and NOAA-20 satellites for high- and normal-confidence intervals only.

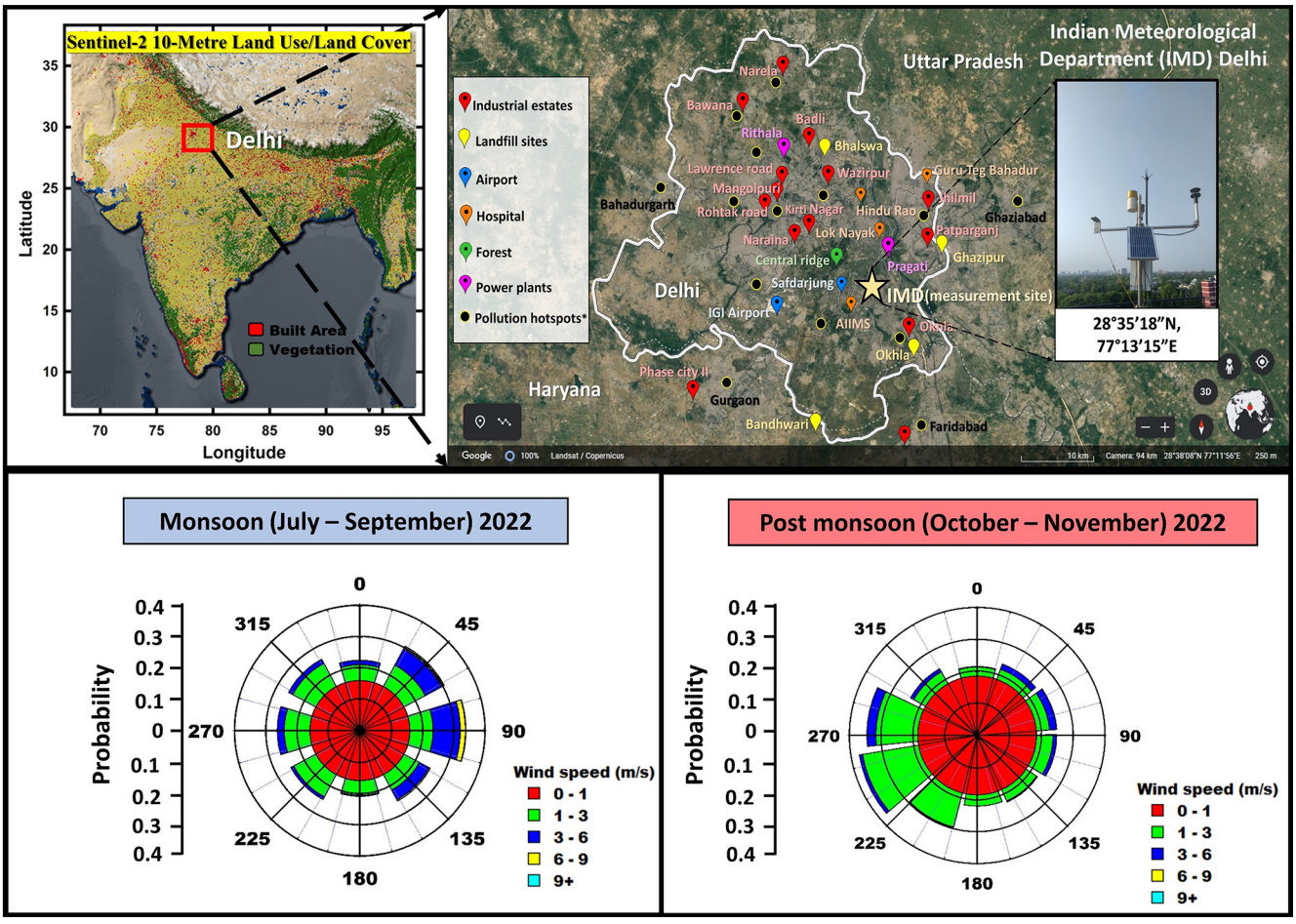

Figure 1. Map of India showing Delhi **(a)** and a zoomed-in view of the measurement site (star) (**b**; Google Earth Imagery © Google Earth), with a view from the rooftop of the SatMet Building (28.5896° N–77.2210° E) and wind rose plots derived from in situ 1 min wind speed and wind direction data during the monsoon **(c)** and post-monsoon **(d)** period of 2022 acquired at sampling height of ∼ 35 m a.g.l.

2.2 Measurement of volatile organic compounds using the PTR-TOF-MS 10K

Volatile organic compounds (VOCs) were measured using a new high sensitivity and high-mass resolution proton transfer reaction time-of-flight mass spectrometer (PTR-TOF-MS 10K; model PT10-004 manufactured by Ionicon Analytik GmbH, Austria). While PTR-TOF-MS 8000 series (Tripathi et al., 2022) and PTR-QMS (Sinha et al., 2014) instruments have been deployed previously in India and have mass resolutions of 8000 and 1, respectively, this study marks the first deployment of the PTR-TOF-MS 10K system in India, a system that possesses several unique advantages over the older-generation instruments for VOC measurements in polluted and complex emission environments. The first is that this new system is equipped with the extended-volatility-range technology (Piel et al., 2021), ensuring that even many intermediate-volatility-range compounds and sticky VOCs can be detected with very fast response times and minimal surface effects. The inlet system of the instrument, as well as the ionization chamber, is fully built into a heated chamber, and the inlet capillary is further fed through a heated hose to ensure there are no "cold" spots for condensation. The entire inlet system is made of inert material (e.g. PEEK- or SilcoNert-treated steel capillaries to keep surface effects minimal). Additionally, a 7 µm SilcoNert filter just before the drift tube served to minimize the clogging/contamination of the system. The second advantage possessed by the PTR-TOF-10K used in this work is the inclusion of an ion booster funnel and hexapole ion guide placed after the drift tube/reaction chamber for improved extraction of ions in a manner that boosts the mass resolution, as well as the sensitivity over its older peers. This helped achieve a much higher mass resolution ($>$ 10 000 m/Δm), even reaching as high as 15 000 m/Δm at m/z 330, and detection limits better than 3 ppt (parts per trillion) for all compounds detected in the mass-to-charge ratio (m/z) 31–330 mass range. These customizations over previously deployed PTR-TOF-MS instruments in Delhi enabled the detection and discovery of several intermediate-range volatile organic compounds (IVOCs)

in the gas phase. Other parts of the instrument have already been explained elsewhere (Jordan et al., 2009; Graus et al., 2011). During this study, the instrument was operated at a drift tube pressure of 3 hPa, drift tube temperature of 120 °C, and drift tube voltage of 470 V, resulting in an operating E/N ratio of ∼ 120 Td (1 Td = 10^{-17} V cm^{-2}). These operational instrumental settings are also summarized in Table S1 in the Supplement.

Ambient air was sampled continuously from the rooftop (∼ 35 m a.g.l.) through a Teflon inlet line that was protected with a Teflon membrane particle filter (0.2 µm pore size; 47 mm diameter) to ensure that dust and debris did not enter the sampling inlet. The length of the inlet line was 5 m and made of Teflon (3 m (0.003 m outer diameter (OD)) and 2 m (0.006 m OD)). The total inlet residence time was ∼ 2.7 s. The part of the inlet that was indoors (3 m (0.003 m OD)) was well insulated and heated to 80 °C. We think this short inlet residence time and heated inlet facilitated the detection of IVOCs relative to previous studies. The instrument background was acquired regularly (typically every 30 min for 5 min) by sampling VOC-free zero air. VOC-free zero air was produced by passing air through an activated charcoal scrubber (Supelpure HC, Supelco, Bellemonte, PA, USA) and a VOC scrubber catalyst (platinum wool) maintained at 370 °C. Mass spectra covering the m/z 15 to m/z 450 range were obtained at 1 Hz frequency. An internal standard comprising 1,3-diiodobenzene ($C_6H_5I_2^+$) detected at m/z 330.848 and its fragment ion ([$C_6H_5I^+$]) detected at m/z 203.943 were constantly injected to ensure accurate mass axis calibration so that any drifts in the mass scale were corrected, providing for accurate peak detection. Primary data acquisition of mass spectra was accomplished using the ioniTOF software (version 4.2; Ionicon Analytik GmbH, 6020 Innsbruck, Austria). All the settings related to PTR (proton transfer reaction), TPS (TOF power supply), MPV (multi-port valve), and MCP (multi-channel plate) can be controlled and optimized using this control software. The raw mass spectra and relevant instrumental metadata are stored in HDF5 format. These spectra were further processed using the Ionicon Data Analytik (IDA version 2.2.0.4; Ionicon Analytik GmbH, Innsbruck, Austria) software that has the functionalities for peak search, peak fits, and preliminary mass assignments and identification of a broad spectrum of organic compounds. The IDA software employs an automated peak detection routine guided by user-defined sensitivity levels for peak detection, peak fit, and shape. The software then uses chemical composition information based on the exact masses and isotopic patterns and calculates a specific proton transfer rate constant (k rate) based on the polarizability and dipole moment for the peaks with an assigned chemical formula instead of using a generic value as was done in previous PTR-TOF-MS measurements in Delhi (Tripathi et al., 2022). We manually compared the values also with the compilation of k rates reported by Pagonis et al. (2019) as an additional check. The user has the possibility of defining a window for mass accuracy (e.g. 30 ppm). Within this defined range and accuracy window, the software identifies all possible chemical compositions and molecular formulae and calculates the corresponding isotope patterns. These patterns are then compared to find the best-fit chemical composition. The process is carried out iteratively, starting with the lower m/z values, according to the method described in the study by Stark et al. (2015).

In this study, a total of 1126 peaks was detected in the raw-measured ambient mass spectra. After further additional quality control and quality assurance steps were performed manually as detailed in Sect. 3, 111 compounds present in ambient air for which the molecular formula could be confirmed unambiguously are reported and for which isotopologues due to molecules of different chemical composition could be ruled out completely were further analysed in this work. The term "unambiguous" is used in the context of the accurate elemental composition/molecular formula assignment of the ions by leveraging the high-mass resolution (8000–13 000 over the entire dynamic mass range) and detection sensitivity (reaching even 1 ppt or better for many ions; see Table S2) of the instrument. This enabled ensuring peaks because expected isotopic signals were not construed as new compounds if their height was exactly as expected for a shoulder isotopic peak based on the natural abundance of isotopes of carbon, hydrogen, nitrogen, sulfur, chlorine, and oxygen that made up the more abundant molecular ion. Where an ion could occur significantly due to fragmentation of another compound, the same has also been noted in Table S2 during attribution of the compound's name. Figure S1 provides an example of visualization of mass spectra and peak assignment using the IDA software, which also illustrates the high-mass-resolving power of the PTR-TOF-MS 10K that enables the separation of ion signals that differ by less than 0.04 Th, as well as the identification of isotopic peaks of parent compounds like methanethiol, dichlorobenzene, C-6 amide, and C-9 carboxylic acid (Fig. S2), which are discussed in detail in Sect. 2.4. Table S2 also provides the limit of detection (LoD) of the compounds, as well as the average and interquartile range observed seasonwise for each ion. The LoD was calculated by taking the 2σ value of the VOC-free zero air instrument background (Müller et al., 2014). Example of measured data showing the instrumental backgrounds and ambient levels for methanethiol, dichlorobenzene, C-6 amide, and C-9 carboxylic acid over a 3 h period are illustrated in Fig. S3. A certified VOC calibration gas mixture (Societa' Italiana Acetilene e Derviati; S.I.A.D. S.p.A., Italy) containing 11 hydrocarbons at ∼ 100 ppb, namely methanol, acetonitrile, acetone, isoprene, benzene, toluene, xylene, trimethylbenzene, and dichlorobenzene and trichlorobenzene, was used during the field deployment for measuring the transmission and sensitivity of compounds covering the mass range ($m/z = 33$ to $m/z = 181$). The instrument was calibrated a total of eight times during the study period on 21 July 2022 after

the first installation, 26 September 2022, 21 October 2022, 26 October 2022, 5 November 2022, 11 November 2022, 16 November 2022, and 30 November 2022. Results were reproducible (~ 21 % or better for all compounds) across all experiments, and a transmission curve obtained from one of the calibration experiments is shown in Fig. S4. Measured transmission further allowed for more accurate quantification by accounting for correction of the mass-dependent detection efficiency of the system. Equation (S1) (de Gouw and Warneke, 2007) was then used to convert the measured ion signals to mixing ratios. The linearity for compounds available in the VOC standard was also checked independently and was above $r \geq 0.9$, as illustrated in Fig. S5 for the tested range of ~ 2 to 8 ppb. The background-corrected concentrations of all the detected m/z were exported from IDA in *.csv format, and further analysis of the data set was carried out using Igor Pro software (version 6.37; WaveMetrics, Inc.). The overall uncertainty calculated using the root mean square propagation of errors due to the accuracy of gas standard and flow controllers was ~ 13 % or better for compounds present in the VOC gas standard. For other compounds reported in this work, it is estimated that the combined accuracy of the transmission function and the parameterized k rates put the overall uncertainty in the range of ± 30 % (Reinecke et al., 2024).

Carbon monoxide (CO) was measured using the IR filter correlation-based spectroscopy air quality analyzer (Thermo Fisher Scientific 48i), while ozone was measured using UV absorption photometry (Model 49i; Thermo Fisher Scientific, Franklin, USA). The overall uncertainty in the measurements was less than 6 %. Details concerning the characterization of the instrument, including calibration and data quality assurance/quality control (QA/QC) protocols, have been comprehensively described in our previous works (Chandra and Sinha, 2016; Kumar et al., 2016; Sinha et al., 2014).

2.3 Mass assignment and compound identification

A total of 1126 peaks was detected in the raw mass spectra. To identify the ambient compounds of relevance in Delhi from these detected peaks, the following additional manual quality control checks were undertaken. First, peaks attributed to non-ambient compounds such as the impurity ions (e.g. NO^+), water cluster ion peaks, and peaks associated with internal standards were excluded, resulting in 1025 peaks for further consideration. Next, the diel profiles and detection limits of these 1025 ion peaks were perused. Only 319 ions out of the 1025 ions showed some diurnal variability and had values above the detection limit after accounting for the respective instrumental background. Next, we verified the presence and expected theoretical magnitude of the shoulder isotopic peaks based on the natural isotopic distribution abundance of the elemental composition of the ion. Figure S6 provides a visual example. This was feasible for all m/z, except the C1 oxygen-containing analyte ions, where the shoulder peak was below the detection limit. The preceding QA/QC resulted in an unambiguous assignment for 111 of the 319 ions. Note that these 111 explained 86 % of the total mass concentration ($\mu g\,m^{-3}$) observed due to the 319 detected peaks when accounting for the isotopic peaks as well. Table S2 lists the ion m/z and molecular formula of the corresponding compound, along with the averaged mixing ratios observed in each case during the monsoon and post-monsoon season. Additionally, the characteristic ambient diel profile classification was one of the following: unimodal, with a daytime peak for biogenic, evaporative, or photochemical source emitted compounds; bimodal, with morning and evening peaks for compounds driven by primary emissions (e.g. toluene); and trimodal, which were a hybrid of the former two, are also provided for each species. Compound names were attributed to specific ions using the assignments reported at m/z in the compiled peer-reviewed PTR-MS mass libraries published by Yáñez-Serrano et al. (2021) and Pagonis et al. (2019), as well as previously published pioneering reports by Stockwell et al. (2015), Sarkar et al. (2016), Yuan et al. (2017), and Hatch et al. (2017).

Fragmentation of certain compounds in specific atmospheric environments can cause significant interferences in the detection of major compounds like isoprene, acetaldehyde, and benzene, as reported recently by Coggon et al. (2024). We also checked these as an additional quality control measure. As noted by Coggon et al. (2024), isoprene can suffer significant interferences from higher aldehydes, as well as substituted cyclohexanes, which can fragment and add to the signal at m/z 69.067 (at which protonated isoprene $C_5H_9^+$ is also detected). The magnitude depends on the instrument operating conditions (Townsend ratio), instrument design, and the mixture of VOCs present in ambient air while co-sampling isoprene. Coggon et al. (2024) very nicely clarified both these aspects and found that when influenced by cooking emissions and oil and natural gas emissions and at higher Townsend ratios, these interferences can be quite significant and even account for up to 50 % of the measured signal attributed to isoprene in extreme cases. We operated the PTR-TOF-MS at 120 Td, which minimizes fragmentation, even if it occurs, compared to when operated at 135–140 Td. Concerning the ambient VOC mixture and emission sources, we note that the type of restaurant cooking emissions present in Las Vegas and over oil and natural gas petrochemical facilities in USA for which Coggon et al. (2024) reported the highest isoprene interferences were absent/negligible at the study site in Delhi. In the latter, open biomass burning sources such as paddy residue burning in post-monsoon season and garbage biomass fires and traffic that occur throughout the year are more significant. Use of more specific though slower analytical techniques based on gas chromatography show that such biomass combustion sources emit significant amounts of isoprene (Andreae, 2019; Kumar et al., 2021). The above points and supporting thermal des-

orption gas chromatography flame ionisation detection (TD-GC-FID) measurements of isoprene, benzene, and toluene (see Fig. S7 and Shabin et al., 2024) led us to conclude that such correction is unwarranted for our PTR-TOF-MS data set. Concerning the interference on acetaldehyde detection due to ethanol, we note that, even in Coggon et al. (2024), this was reported to only be of significance in highly concentrated ethanol plumes such as those encountered on the Las Vegas strip, where ~ 1500 ppb of ethanol was detected. On the contrary, in Delhi, as listed in Table S2, ethanol values detected at m/z 47.076 were on average only 0.2 ppb (interquartile range 0.16 ppb) during monsoon and 0.55 ppb (interquartile range 0.5 ppb) in the post-monsoon season, respectively, whereas acetaldehyde detected at m/z 45.03 was significantly higher at 3.34 and 7.75 ppb during the monsoon and post-monsoon seasons, respectively.

For the same molecular formula, several isomeric compounds with differing chemical structures are possible, with the number of possibilities increasing enormously with an increase in the number of atoms that make up the molecule. In addition, in some instances, fragmentation of other compounds can complicate the compound attribution for a given ion. Nonetheless, in the interest of stimulating interest and further investigation, as many have been previously rarely reported or are being reported for the first time in ambient air, we have provided one of the many possible chemical structures in bold in Table S2. We do caution that the chemical structure provided by no means even constitutes a best-guess estimate but nonetheless would be appealing to chemists and provoke further detailed reporting rather than just the molecular formula.

3 Results and discussion

3.1 Analyses of ambient mass spectra and mass concentration contributions of VOC chemical classes

A summary of the distribution of the 111 compounds in terms of chemical classes showing their averaged measured ambient mass concentration ($\mu g\,m^{-3}$) contributions is shown in Fig. 2 for the monsoon (22 July–30 September 2022) and post-monsoon seasons (1 October–26 November 2022). Out of the 111 compounds, 42 were pure hydrocarbons made up only of carbon and hydrogen atoms; 56 were oxygenated volatile organic compounds (OVOCs) made up of only carbon, hydrogen and oxygen; 10 contained nitrogen (NVOCs); 2 contained chlorine (ClVOCs); and 1 contained sulfur (SVOC). The average total mass concentration of the same set of pure hydrocarbons during post-monsoon season was 3.7 times greater than in monsoon season ($40\,\mu g\,m^{-3}$ vs. $148\,\mu g\,m^{-3}$), while the average total mass concentration of OVOCs during post-monsoon was 2.6 times greater than the monsoon season values ($44\,\mu g\,m^{-3}$ vs. $116\,\mu g\,m^{-3}$). Pure hydrocarbons and OVOCs contributed similarly to the mass concentrations in monsoon season, but during the post-monsoon season, the contribution of pure hydrocarbons was significantly higher than that of OVOCs due to an increase in the primary emissions of these compounds. The average mass concentration of NVOCs during post-monsoon was thrice as high relative to the monsoon season (1 and $3\,\mu g\,m^{-3}$). For the chlorine-containing VOCs, the post-monsoon concentrations were 20 times higher, though in absolute magnitude, the values were low ($1\,\mu g\,m^{-3}$). The average mass concentration of sulfur-containing VOCs during post-monsoon was 4 times higher, but again, absolute values were low ($0.2\,\mu g\,m^{-3}$). The top 10 pure hydrocarbon compounds by mass concentration ranking were toluene, the sum of C8 aromatics (xylene and ethylbenzene isomers), propyne, 1-butene, benzene, the sum of C9 aromatics (trimethyl benzene isomers), propene, the sum of monoterpenes, isoprene, and 1,3 butadiene and contributed to 84 % of the total mass concentration due to pure hydrocarbons during both the monsoon and post-monsoon seasons, respectively, while the top 20 contributed to 95 % and 96 % of the total mass concentration in monsoon and post-monsoon seasons, respectively. The top 10 OVOCs include methanol, acetone, acetic acid + glycolaldehyde, acetaldehyde, hydroxyacetone, formaldehyde, 2-butanone, 2,3-butanedione, formic acid, and butanoic acid, which collectively contributed to 84 % and 79 % of the total mass concentration due to all OVOCs in the monsoon and post-monsoon seasons, respectively, while the top 20 contributed to 93 % and 90 % of the total mass concentration in the monsoon and post-monsoon seasons, respectively.

The top four NVOCs, namely acetonitrile, nitroethane, formamide, and isocyanic acid, contributed to 92 % and 91 % of the total mass concentration in the monsoon and post-monsoon seasons, respectively. Out of two identified chlorine-containing VOCs, dichlorobenzene ($C_6H_4Cl_2$) was found to be the major contributor, contributing 87 % and 95 % of the total mass concentration in the monsoon and post-monsoon seasons, respectively. The only sulfur-containing VOC was methanethiol [CH_4S], and it was detected at its protonated ion m/z 49.007 and confirmed by the shoulder isotopic peak. Overall, there was an increase in the mass concentration of all the classes of VOCs from monsoon to post-monsoon. This increase in mass concentration could be attributed to increased emissions from sources that get active in the post-monsoon period, such as regional post-harvest paddy residue burning and increased open waste burning, as well as a reduced wet scavenging and ventilation coefficient compared to the monsoon season. We examine these in more detail in the next sections.

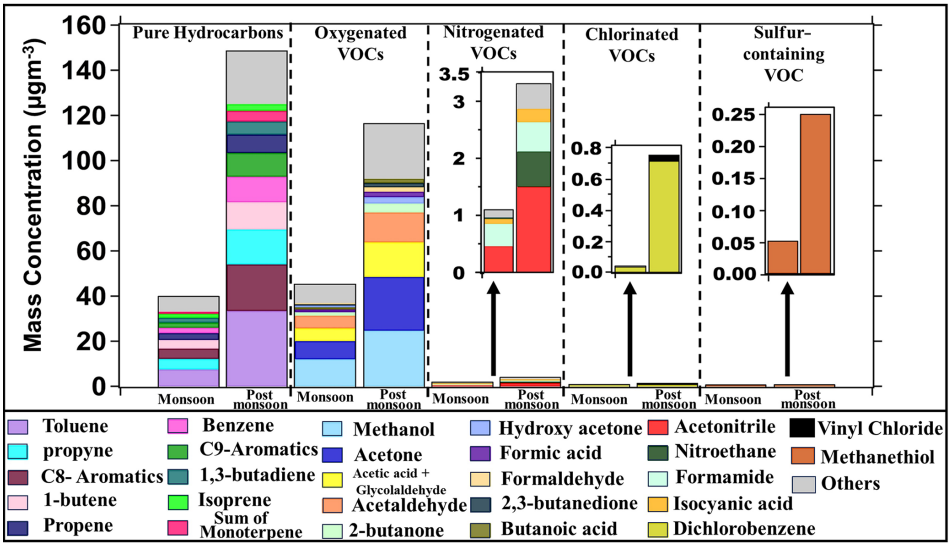

Figure 2. Bar graph of 111 compounds class-wise, namely pure hydrocarbons, oxygenated VOCs (OVOCs), nitrogen-containing VOCs (NVOCs), chlorine-containing VOCs (ClVOCs), and sulfur-containing VOC (SVOC) in both monsoon and post-monsoon periods.

3.2 Time series of VOC tracers during the "clean" monsoon and "polluted post-monsoon" seasons in Delhi

Figure 3 shows the time series plot of meteorological parameters and the mixing ratios of some key VOC tracer molecules during monsoon (22 July–30 September 2022; shaded blue region) and post-monsoon (1 October–26 November 2022; shaded red region). The top panel shows the ambient temperature (°C), with the daily VIIRS fire counts on the left-hand side of the top panel and the ventilation coefficient ($m^2\ s^{-1}$) and daily rainfall (mm) on the right-hand side of the top panel during the study period (22 July–26 November 2022). A grid (1 km × 1 km) with latitudes between 21 and 32° N and longitudes between 78 and 88° E was considered for extracting the fire count data. The second panel from the top represents the time series of the mixing ratios of OVOCs, which can be formed photochemically and be emitted from anthropogenic sources, namely methanol, acetaldehyde, and the sum of acetone and propanal. The third panel shows the mixing ratio of isoprene (a daytime biogenic chemical tracer and pure hydrocarbon) and photosynthetic active radiation (PAR) (µmol photons $m^{-2}\ s^{-1}$), and the fourth panel shows the mixing ratio of acetonitrile (a biomass burning chemical tracer) and furan (a combustion chemical tracer). The bottom panel shows the mixing ratios of benzene, toluene, the sum of C8 aromatics (xylene and ethylbenzene isomers), and the sum of C9 aromatics (trimethylbenzene and propyl benzene isomers). These are some of the most abundant VOCs typically present in any urban megacity environment due to their strong emission from traffic and industries, in addition to biomass burning (Sarkar et al., 2016; Sinha et al., 2014; Chandra et al., 2016; Singh et al., 2023; Dolgorouky et al., 2012; Yoshino et al., 2012; Langford et al., 2010). We note that all the meteorological conditions and fire activity and VOC levels changed significantly between the much "cleaner" monsoon season and "highly polluted" post-monsoon season at the same site. While the average temperature during monsoon season was 29.5 ± 2.8 °C, in the post-monsoon season this changed to 24.8 ± 5.2 °C, and the average ventilation coefficient was 1.7 times higher during the monsoon season relative to the post-monsoon season. Except for the period impacted by heavy rainfall due to western disturbance weather (8–10 October 2022), the average mixing ratios for all compounds were considerably higher in the post-monsoon season relative to the monsoon season, even after accounting for the ventilation coefficient reduction with all the aromatic compounds like benzene; toluene; the sum of C8 and C9 aromatics, all 4.5 times higher; furan, more than 5 times higher; acetonitrile; acetone, more than 3 times higher; and methanol and acetaldehyde 2 times higher. Even isoprene was 1.7 times higher, but its nighttime mixing ratios were higher than the daytime mixing ratios during the post-monsoon season relative to the monsoon season. The increases clearly exceed what can be accounted for only by the reduced ventilation coefficient (seasonality) and suggests an increase in anthropogenic combustion-related sources in particular from open biomass burning fire sources, which we investigate in more detail in the subsequent sections.

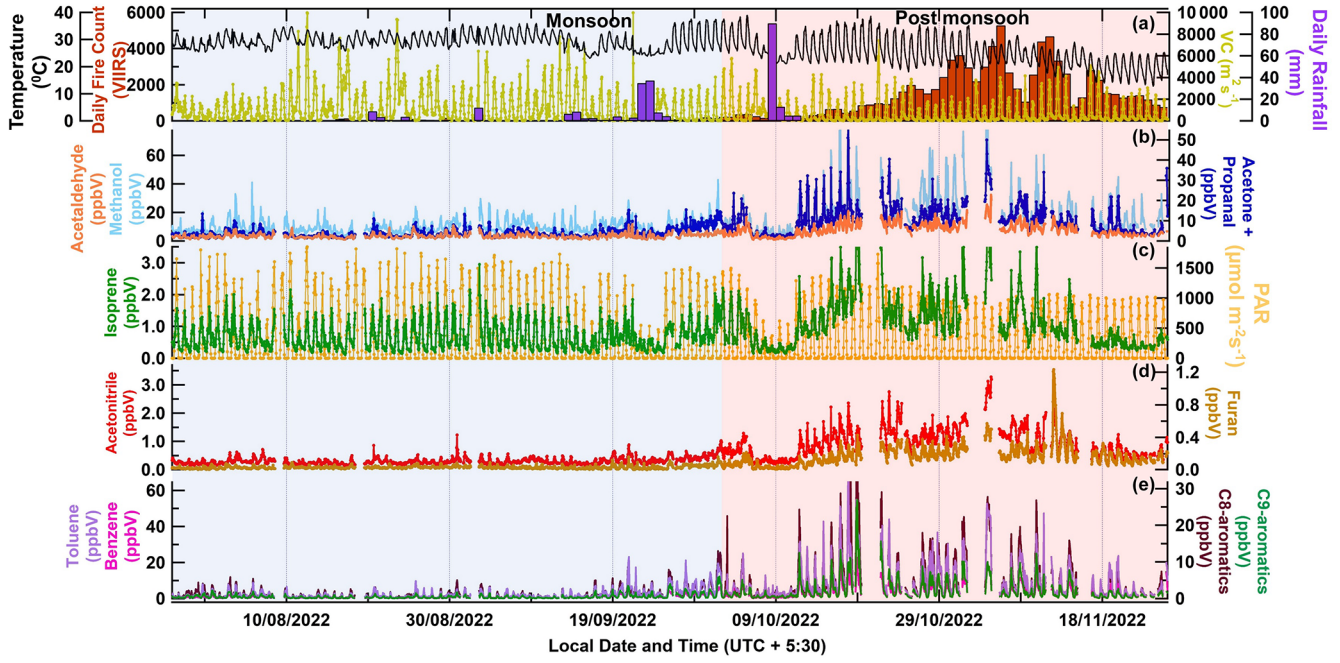

Figure 3. Time series of hourly data for meteorological parameters like temperature (°C) and ventilation coefficient ($m^2\ s^{-1}$), daily rainfall, and daily fire counts **(a)**. Hourly mixing ratios of methanol, acetaldehyde, and the sum of acetone and propanal **(b)**. Isoprene and PAR ($\mu mol\ m^{-2}\ s^{-1}$) **(c)**. Acetonitrile and furan **(d)**. Benzene, toluene, and the sum of C8 aromatics (xylene and ethylbenzene isomers) and the sum of C9 aromatics (isomers of trimethyl benzene and propyl benzene) **(e)**. The shaded blue and red regions represent the monsoon and post-monsoon periods, respectively.

3.3 Analyses of the diel profiles during the "clean" monsoon and "polluted post-monsoon" seasons in Delhi for discerning major drivers of their ambient values

Figure 4 shows the diel box-and-whisker plot depicting the average, median, and variability (10th, 25th, 75th, and 90th percentile) of the same key VOCs like methanol, acetonitrile, acetaldehyde, acetone and propanal, furan, isoprene, benzene, toluene, and C8 aromatics for monsoon (derived from ∼ 1704 data points; blue markers) and post-monsoon (derived from ∼ 1368 data points; red markers) against the hour of the day (the horizontal axis represents the start time of the corresponding hourly bin). This more clearly brings out the season-wise diel variation in the compounds and in turn throws light on the emission characteristics and how they vary for the same compound between seasons. Both in the monsoon and post-monsoon season, methanol mixing ratios seem to be driven by primary emission sources and correlate very well with toluene, a tracer for traffic emissions, with highest increases in the evening hours (17:00 to 20:00 LT). Globally, the main source of methanol is vegetation, but in a megacity like Delhi that possesses more than 150 000 compressed natural gas (CNG) vehicles and light-duty diesel vehicles, it appears that traffic-emitted (see Fig. 1 of Hakkim et al., 2021) methanol controls its ambient abundance. Similarly, based on the correlation with toluene, traffic emissions seem to be a major contributor for acetaldehyde, acetone, the sum of C8 aromatics, and benzene in the morning and evening hours. All of these compounds are among the most abundant VOCs detected in tailpipe exhaust samples (Hakkim et al., 2021). Average ambient mixing ratios of acetonitrile, a compound emitted significantly from biomass burning (Holzinger et al., 1999), were below 0.5 ppb in the monsoon season for all hours, with only a slight increase at night, but during post-monsoon season, the values doubled to 1 ppb for all hours, with strong increases in the early evening and nighttime hours. This tendency was mirrored in all the other compounds including isoprene. The diel profiles of isoprene and acetaldehyde were the only ones which showed daytime maxima during the monsoon season.

This shows that during the monsoon season, the biogenic sources of isoprene majorly drive its ambient mixing ratios, whereas acetaldehyde ambient mixing ratios are controlled by photochemical production of the compound in the monsoon season. Under the high NO_x conditions prevalent in a megacity like Delhi, photooxidation of *n*-butane, propene, ethane, and propane could be a large photochemical source of acetaldehyde (Millet et al., 2010).

Benzene, which is a human carcinogen is the only VOC for which there is a national ambient air quality standard ($5\ \mu g\ m^{-3}$ equivalent to ∼ 1.6 ppb at 298 K) in India. Average mixing ratios in the post-monsoon season (Fig. 4) were

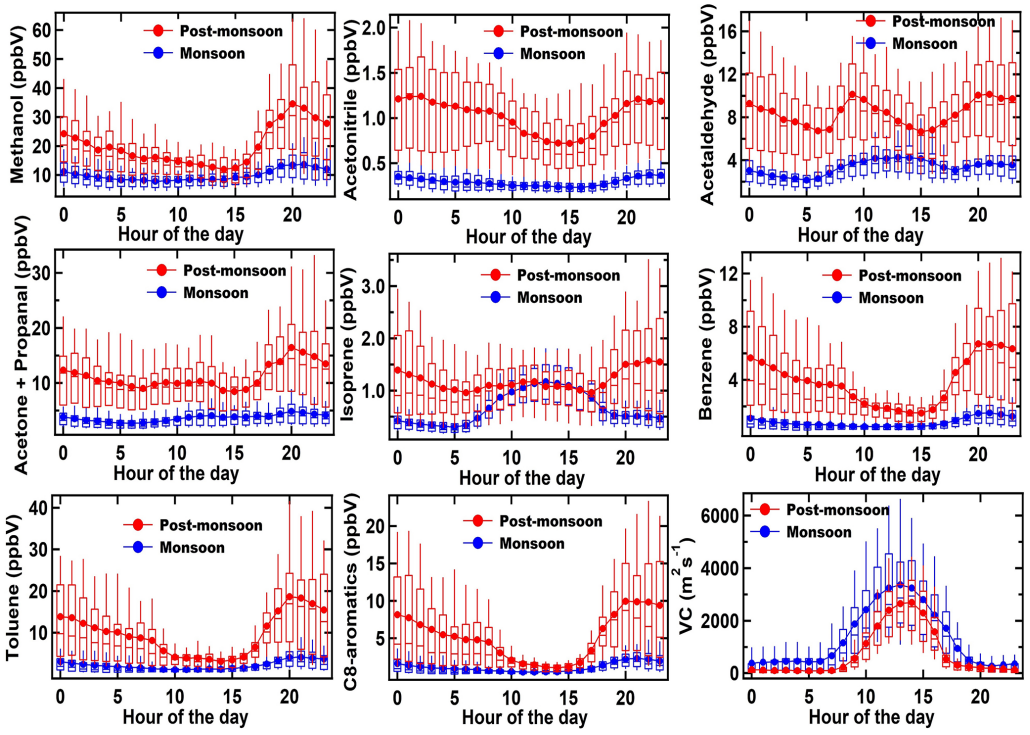

Figure 4. Box-and-whisker plots showing average, median, and variability (10th, 25th, 75th, and 90th percentile) for some major VOCs and the ventilation coefficients ($m^2\ s^{-1}$) (VC) during the monsoon and post-monsoon periods. The blue and red markers represent the monsoon and post-monsoon periods, respectively.

always above this value no matter what hour of the day it was, and the seasonal average was twice as high as this value (∼ 4 ppb). The increased biomass burning in the post-monsoon season controlled the abundance of benzene, acetaldehyde, acetone, and isoprene during this period, due to the strong emissions from both biomass burning and traffic. The typical atmospheric lifetimes of all these compounds spans from a few hours (e.g. isoprene) and several days (e.g. benzene and methanol) to several months in the case of acetonitrile. The results of the TD-GC-FID measurements, along with the average PTR-TOF-MS values presented in Fig. 4, are summarized in Fig. S7. Even though the TD-GC-FID measurements present only a snapshot, as the ambient sampling duration is shorter, the season-wise diel profiles are consistent with those obtained using the PTR-TOF-MS, and the average mixing ratios obtained using the PTR-TOF-MS data set also fall well within the range of mixing ratios observed using the TD-GC-FID. This provides further confidence in the high nighttime isoprene observed during the post-monsoon season. The isoprene emissions at night during the post-monsoon season are likely due to combustion sources. Paddy residue burning and dung burning have the highest isoprene emission factors of $\sim 0.2\ g\ kg^{-1}$ (Andreae, 2019), and more than 8 Gg of isoprene is released regionally in the space of a few weeks during the post-monsoon season from open-paddy residue burning alone (Kumar et al., 2021). Previous studies from the region have also documented isoprene emissions from non-biogenic sources, which are also active at night (Kumar et al., 2020; Hakkim et al., 2021). In 2018, at another site in Delhi, using gas chromatography measurements made in the pre-monsoon and post-monsoon periods, Bryant et al. (2023) reported average nocturnal mixing ratios of isoprene that were 5 times higher in the post-monsoon compared to the pre-monsoon and showed different diel profiles between the seasons. They found that the high nighttime isoprene correlated well with carbon monoxide, a combustion tracer, and suspected that in addition to the stagnant meteorological conditions, biomass burning sources could be a reason for the significant nighttime isoprene in Delhi in the post-monsoon season. Our findings, using more comprehensive and high temporal resolution data, further substantiate the surprising nighttime isoprene.

As potent precursors of secondary organic aerosol, the aromatic compounds would also enhance secondary organic aerosol pollutant formation during the polluted post-monsoon season. When compared with the first PTR-MS measurements of these compounds reported from wintertime Delhi (see Fig. 2 in Hakkim et al., 2019), the average levels of these compounds for the post-monsoon season (Table S2) are lower or comparable but still significantly higher than what has been reported for other major cities of the world like Tokyo, Paris, Kathmandu, Beijing, and London (Yoshino et

al., 2012; Dolgorouky et al., 2012; Sarkar et al., 2016; Li et al., 2019; Langford et al., 2010). The monsoon levels, on the other hand, were comparable to many of the other megacities.

As the monsoon season is characterized by favourable meteorological conditions for wet scavenging and dispersal due to a higher ventilation coefficient, as well as significantly lower open biomass burning due to wet and warm conditions, the monsoon levels can be considered baseline values for the ambient levels of these compounds (except isoprene and acetaldehyde) in Delhi, which are driven mainly by year-round traffic and industrial sources in Delhi. During the monsoon season, the major drivers for isoprene emissions are biogenic sources, whereas for acetaldehyde, the major driver is photochemistry, a finding that is similar to what has been reported previously from another site in the Indo-Gangetic Plain (Mishra and Sinha, 2020).

3.4 Discovery of methanethiol (CH_3SH), dichlorobenzenes ($C_6H_4Cl_2$), C6 amides ($C_6H_{13}NO_2$), and C9 organic acids ($C_9H_{18}O_2$) in ambient Delhi air

Figure 5 shows the average diel profile of four compounds present in both the monsoon and post-monsoon periods that have, to our knowledge, never been reported from Delhi or any site in South Asia and have only rarely been reported in the gas phase in any atmospheric environment in the world. Except for methanethiol detected at m/z 49.007 (also called methyl mercaptan), all the other compounds, namely dichlorobenzene ($C_6H_4Cl_2$) detected at m/z 146.977, C6 amides like hexanamide ($C_6H_{13}NO_2$) and its isomers detected at m/z 116.108, and C9 carboxylic acid/ester such as nonanoic acid ($C_9H_{18}O_2$) and its isomers detected at m/z 159.14, are all intermediate-volatility-range organic compounds. The saturation mass concentration (C_0) of methanethiol, C6 amide, dichlorobenzene, and C9 organic acid, were calculated using the method described in Li et al. (2016), using the following equation:

$$C_0 = \frac{M\,10^6\,p_0}{760\,R\,T}, \quad (1)$$

wherein M is the molar mass [g mol^{-1}], R is the ideal gas constant [8.205×10^{-5} atm K^{-1} mol^{-1} m^3], p_0 is the saturation vapour pressure [mm Hg], and T is the temperature (K). Organic compounds with $C_0 > 3 \times 10^6$ µg m^{-3} are classified as VOCs, while compounds with $300 < C_0 < 3 \times 10^6$ µg m^{-3} as intermediate VOCs (IVOCs).

The presence of such reactive organic sulfur-, chlorine-, and nitrogen-containing compounds in the gas phase provides new insights concerning the chemical composition and secondary chemistry occurring in air during the extremely high-pollution events. Below, we examine the sources and chemistry of these compounds in further detail.

The diel profiles of both methanethiol and dichlorobenzene in both the monsoon and post-monsoon seasons were similar (bimodal with afternoon minima) and controlled by the ventilation coefficient diel variability (see Fig. 4), and in fact, even the difference in their average magnitudes (50 ppt vs. 130 ppt for CH_3SH and 25 ppt vs. 100 ppt for dichlorobenzene between monsoon and post-monsoon seasons) can largely be explained by the reduction in the ventilation coefficient (~ 2 reduction). Furthermore, the conditional probability wind rose plots for both compounds shows that the high values come from the same wind sector upwind of the site spanning the northeast to south during early morning and evening hours, which is actually where a variety of industrial sources are located. Previously, Nunes et al. (2005) and Kim (2006) have reported methanethiol from petrochemical industries and landfills in Brazil and Korea, respectively. Toda et al. (2010) reported high (tens of parts per billion) methanethiol mixing ratios from a pulp and paper mill industry in Russia.

Both compounds are also used in the deodorant and pesticide products as reagents (Chin et al., 2013), and although large-scale pesticide manufacturing facilities were shifted out of Delhi, there are still units that sell and distribute these products in those areas from which fugitive emissions are likely happening. Methanethiol is further used as a precursor in methionine production (François, 2023), an essential amino acid used in manufacture of pesticides, and the fragrance industry uses methanethiol for its distinct sulfur-like aroma (Bentley and Chasteen, 2004), contributing to the creation of savoury flavours and unique fragrances. In the Delhi environment, a combination of such industries, in particular paper and pulp industries, likely forms candidate sources. Figure 5 confirms that elevated methanethiol values in the wind rose had a clear directional dependence from the area spanning the northern to southeastern sector. This is the region where various manufacturing facilities and industrial areas of Delhi like Patparganj (northeast) Okhla, Faridabad (south) are situated, and these industrial estates were marked earlier in Fig. 1b. Methanethiol is an extremely reactive molecule, reacting primarily with the hydroxyl radical (OH) during daytime, with an estimated lifetime of 4.3 h (Wine et al., 1981). Its photooxidation in the daytime with hydroxyl radicals produces sulfur dioxide, methanesulfonic acid, dimethyl disulfide, and sulfuric acid (Kadota and Ishida, 1972; Hatakeyama and Akimoto, 1983), all of which play key roles in aerosol formation pathways. Dimethyl disulfide has a very short atmospheric lifetime, spanning from 0.3 to 3 h (Hearn et al., 1990), because of its high reactivity ($[1.98 \pm 0.18] \times 10^{-10}$ cm^3 molec.$^{-1}$ s^{-1}) (Wine et al., 1981) with OH radicals. Although dimethyldisulfide is the major product of the photooxidation of methanethiol (yield 50 %; Wine et al., 1981), since methanethiol itself was on average only 48 ppt (monsoon) and 128 ppt (post-monsoon), and plumes occur only at night, we hypothesize that the ambient concentrations of dimethyl disulfide (DMDS) were too

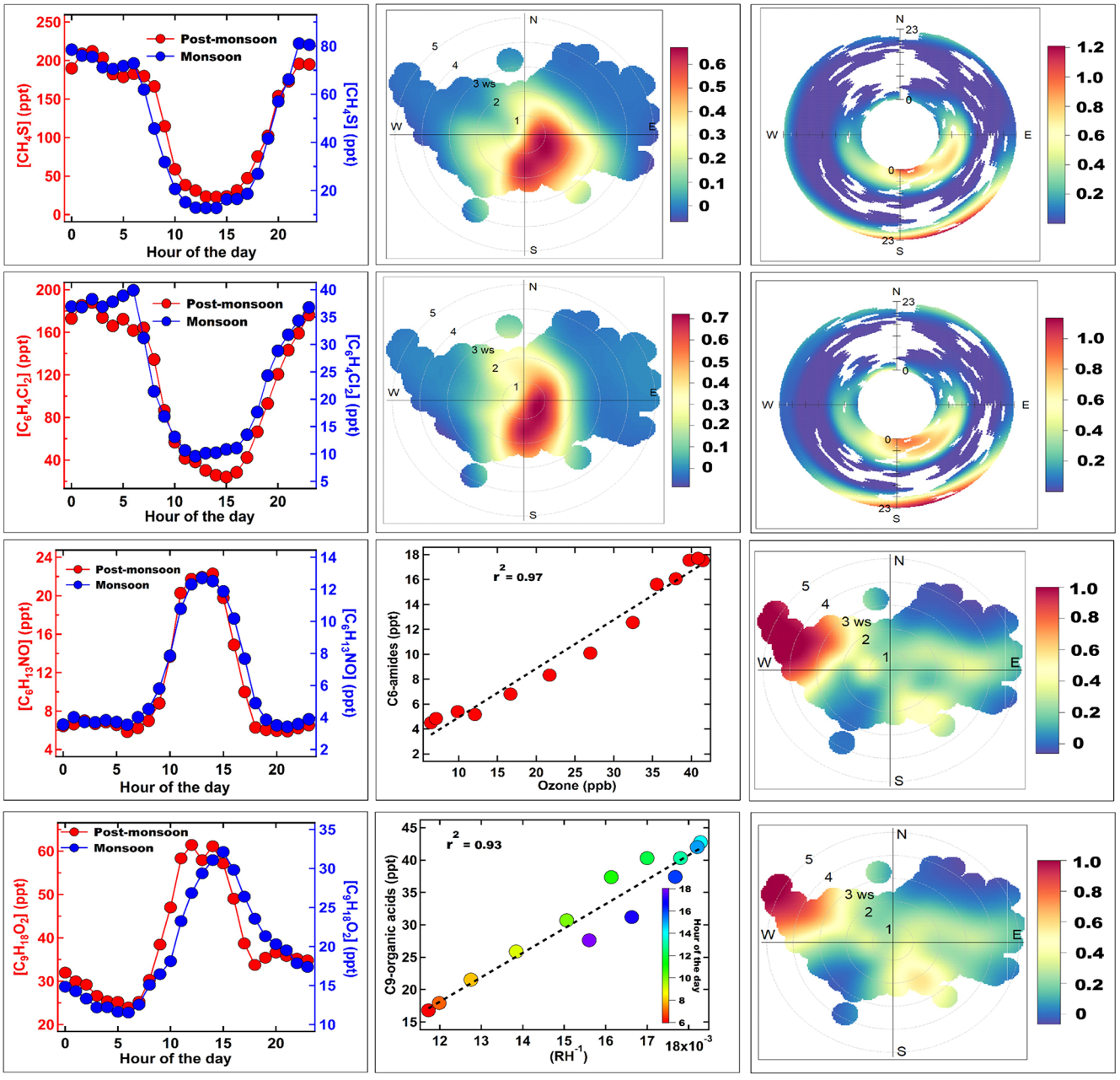

Figure 5. Average diurnal profile of methanethiol, isomers of dichlorobenzene, C6 amides, and C9 organic acid in the left panel for both the monsoon (blue marker) and post-monsoon (red marker) periods. The second panel shows the wind rose plot of methanethiol and isomers of dichlorobenzene, a plot of C6 amide vs. ozone, and C9 organic acid vs. RH^{-1} colour coded by the hour of the day. The third panel shows the polar annulus plot of methanethiol and isomers of dichlorobenzene and a wind rose plot of C6 amides and C9 organic acid.

low to be detected by the mass spectrometer. Furthermore, it can also react with nitrate radicals (Berreshiem et al., 1995) and participate in nighttime chemistry. More recently, Reed et al. (2020) performed laboratory experiments and observed that even trace amounts of organosulfur compounds, such as thiols and sulfides, can significantly enhance the organic aerosol mass concentration and its particle effective density. Though there has not been any relevant data set attributing the enhancement of organic aerosols to methanethiol in Delhi specifically, previous studies have found enhanced secondary aerosol formation rates during haze and fog episodes (Acharja et al., 2022). These studies collectively suggest an increase in the haze events in Delhi is linked to sulfur chemistry in which methanethiol, due to its high reactivity and atmospheric chemistry, could also be a contributor, along with ammonia and other sulfur-containing molecules. Wine

et al. (1981) had further predicted that the very rapid rate at which methanethiol reacts with OH would result in low steady-state concentrations in ambient air, even though reasonably large-scale sources may exist.

Several recent studies have reported high chloride in the sub-micron aerosol of Delhi (Gani et al., 2020; Acharja et al., 2023; Pawar et al., 2023). Dichlorobenzene is an intermediate-range volatile organic compound (IVOC) which can partition between gas and aerosol phase. However, to date, no gaseous IVOC chlorinated organic compounds have been reported in ambient air from India. *p*-dichlorobenzene (PDCB), also called 1,4-dichlorobenzene, is one of the dichlorobenzene isomers known for its use as a pest repellent and deodorant in indoor environments. 1,4-dichlorobenzene in outdoor air in various locations in North America and Europe ranged from 30 to 830 ppt (Chin et al., 2013). It is emitted only from anthropogenic sources, as there are no known natural sources. Its emission sources include consumer and commercial products containing PDCB, waste sites, and manufacturing facilities for flavour and as insect repellent products (ATSDR, 2006). Its atmospheric lifetime is estimated to be 21–45 d (Mackay et al., 1997). It has been reported as a precursor of secondary organic aerosol in indoor conditions (Komae et al., 2020). Due to its long lifetime, dichlorobenzene can be transported to upper regions of the atmosphere, where release of some reactive chlorine through photolysis can occur, but this is not likely to be of great consequence. Instead, reaction with hydroxyl radicals would convert it more readily to phenolic compounds that would readily partition to aqueous aerosol phase and also undergo nitration to form nitrophenols (Hu et al., 2021), which are a component of brown carbon (Lin et al., 2015, 2017).

In contrast, the diel profile of the average mixing ratios of $C_6H_{13}NO$ (Fig. 5), likely hexanamide or isomers of C6 amides measured at m/z 116.108, was similar in both the monsoon and post-monsoon seasons and characteristic of a compound with a purely photochemical source with no evening peaks, even during the enhanced biomass burning in the post-monsoon season. As observed for several other compounds in this study, the difference in the magnitude between both seasons (peak value 22 ppt in the post-monsoon season vs. 12 ppt in the monsoon season) could be accounted for almost completely by the reduced ventilation coefficient in the post-monsoon season (factor of ~ 2). The presence of photochemically formed formamide and acetamide from OH oxidation of alkyl amine precursors has been reported previously (Chandra et al., 2016; Kumar et al., 2018) from another site in the Indo-Gangetic Plain which experiences strong agricultural waste burning. In the literature, we could find only one report on the presence of C6 amides in the ambient air in the gas phase in Yao et al. (2016), who reported ~ 14 ppt in the summertime air of Shanghai using an ethanol reagent ion chemical ionization mass spectrometer (CIMS), the source of which was both industrial and photochemical in origin. However, to our knowledge, this is the first study worldwide to detect and report only photochemically formed C6 amides in the gas phase. C6 amides are IVOCs, which can easily partition to aerosol phase, depending on environmental conditions and also act as a new source of reactive organic nitrogen to the atmospheric environment. We found the highest values in air masses arriving in the afternoon from the northwestern direction at high wind speeds (see Fig. 5) during the post-monsoon season, which indicated that paddy stubble burning emissions of amines (Kumar et al., 2018) were its likely precursors. The mechanism of amide formation through photochemical reactions has been elucidated in several previous laboratory studies (Bunkan et al., 2016; Barnes et al., 2010; Nielsen et al., 2012; Borduas et al., 2015). When correlated with daytime ozone hourly mixing ratios, the very high correlation ($r^2 > 0.97$) confirmed its purely photochemical origin. Being an amide, further gas phase oxidation products are likely to result in organic acids or condensation on existing aerosol particles, which could add to the reactive organic nitrogen in aerosol phase and neutralize the acidity just like ammonia, as ammonium ion is formed from hydrolysis of amides (Yao et al., 2016). However, the exact role of these amides in nucleation and aerosol chemistry will warrant further investigation.

Finally, the last row of Fig. 5 shows the average mixing ratios of the compound with molecular formula $C_9H_{18}O_2$, which is likely due to isomers of C9 carboxylic acids (e.g. nonanoic acid), although one cannot rule out contributions from isomers of esters such as methyl octanoate or 2-methylbutyl isobutyrate also detected at m/z 159.14. Von Hartungen et al. (2004), and more recently the study by Salvador et al. (2022), have highlighted that carboxylic acids (RCOOH) can undergo dissociation reactions within the drift tube in addition to protonation and form acylium ions as per the following reactions (von Hartungen et al., 2004):

$$H_3O^+ + RCOOH \rightarrow RCOOHH^+ \text{ (protonated ion)} + H_2O, \quad \text{(R1)}$$

$$H_3O^+ + RCOOH \rightarrow RCO^+ \text{ (acylium ion)} + 2H_2O. \quad \text{(R2)}$$

We detected the corresponding acylium ion of C9 carboxylic acid ($C_8H_{17}CO^+$ detected at m/z 141.13) in the measured ambient spectra (Fig. S9) and found that not only was it present but that it also correlated well in the ambient data with the protonated ion ($r = 0.83$). The presence of the fragment ion and its correlation provides an additional confirmation concerning the attribution of m/z 159.14 to the C9 organic acid, and a quantification of the ion signals due to the protonated and acylium ions were summed together for greater accuracy. Although here also there is a daytime peak, the timing of the peak is much later in the day (15:00 LT). The peak hourly values reached 60 ppt in post-monsoon season. It showed a high correlation ($r^2 > 0.93$) with the inverse of the ambient daytime relative humidity, indicating that it partitions back and forth between the gas phase and aerosol phase, depending on the environmental conditions of temper-

ature and RH. *n*-alkanoic acids in general and nonanoic acid in particular have long been reported as major organic acids present in biomass burning emitted organic aerosol (Oros et al., 2006; Fang et al., 1999). The corresponding wind rose plot (Fig. 5) shows that the highest values were in air masses arriving at high wind speeds in the afternoon from the northwest during post-monsoon season, which is a major source region of biomass burning emitted organic aerosols. It is also possible that photochemical oxidation through ozonolysis of precursors and hydroxyl radical initiated oxidation can form such carboxylic acids as an advanced oxidation product (Kawamura et al., 2013). In both cases, biomass burning emissions and evaporation from the aerosol phase appear to be the major source of this compound. Carboxylic acids in the aerosol phase would serve to neutralize some of the excess ammonia in the atmospheric environment of the Indo-Gangetic Plain (Acharja et al., 2022) and would be important for nighttime aerosol chemistry in Delhi.

3.5 Comparison of ambient mixing ratios and VOC / CO emission ratios for aromatic VOCs in Delhi with some megacities of Asia, Europe, and North America

Aromatic compounds are among the most important class of compounds in urban environments due to their direct health effects (e.g. benzene is a human carcinogen) and reactivity as ozone and secondary organic aerosol precursors. Therefore, these compounds have been widely investigated in many cities, and information concerning their ambient levels and emission ratios to carbon monoxide is often used for assessing similarities and differences in the sources of these compounds in varied urban environments (Warneke et al., 2007; Borbon et al., 2013). In Fig. 6, we show the emission ratios (ERs) derived for benzene, toluene, and the sum of C8 and C9 aromatic compounds (VOC / CO ppb/ppm) using nighttime monsoon (left panel) and post-monsoon (right panel) measurements made in Delhi. The method is based on a linear regression fit to determine the slope of the nighttime scatterplot data (from 20:00 to 06:00 LT) between a VOC (ppb) and CO (ppm) (de Gouw et al., 2017; Borbon et al., 2013). Using nighttime hourly data (18:00 to 06:00 LT) provides the advantage of minimizing complications due to daytime oxidative losses of the compounds. It can be noted from Fig. 6 that during the monsoon season (from 18:00 to 23:00 and 00:00 to 06:00 LT) and the post-monsoon season (18:00 to 23:00 LT), the observed emission ratios as inferred from the slopes and fits are not statistically different from each other (all highlighted by oval circles) with values for benzene / CO, toluene / CO, the sum of C8 aromatics, and the sum of C9 aromatics / CO in the range of 1.2–2.43, 3.14–6.76, 1.97–3.84, and 1.05–2.07, respectively. All these emission ratios fall within the range of what has been reported for typical petrol two- and four-wheeler vehicles in India in tailpipe emissions (Hakkim et al., 2021). For the monsoon season, although two linear fits are observed from 18:00 to 23:00 and 00:00 to 06:00 LT, the values of the emission ratios, as inferred from the respective slopes, for all compounds overlap or are very close to each other and within the uncertainties for all compounds. We hypothesize that the two fits are due to the change in relative numbers of two-wheelers and four-wheelers. In the post-monsoon season, however, for the time period in the second half of the night (00:00–06:00 LT), the emission ratios derived from the slopes are statistically different from the ones observed in monsoon season and the first half of night in post-monsoon season (18:00–23:00 LT). When we examined the wind rose plots for the same nighttime data of the aforementioned compounds for each season (Fig. S8), we noted that during the post-monsoon season more pollution plumes from the southeastern sector, which has industrial facilities, and the northwestern sector (a major fetch region for biomass burning plumes from regional paddy residue burning in Punjab and Haryana) occurred. During the post-monsoon season due to dip in temperatures at night, the heating demand (Awasthi et al., 2024) and associated open biomass burning (Hakkim et al., 2019) also goes up, relative to the monsoon period nights. Hence, overall, we think that these additional sources in the post-monsoon season do add to the burden of these mainly traffic emitted aromatic compounds and could help explain – at least partially – the higher emission ratios observed during the post-monsoon season (00:00–06:00 LT), wherein values for benzene / CO, toluene / CO, the sum of C8 aromatics, and the sum of C9 aromatics / CO values range from 3.15–3.27, 7.72–8.68, 5.03–5.37, and 2.6–2.76, respectively, and are statistically different from the others (the ones marked by oval circles).

Table 1 provides a comparison of the ambient mixing ratios and emission ratios that have been reported in some other major megacities of Asia, Europe, and North America for these compounds. Although the year of measurement and seasons are not the same, such a comparison nonetheless helps to put the 2022 levels of these compounds in Delhi in a global context. It may be further noted that we took care to calculate the emission ratios using only nighttime data when chemical loss of these compounds is negligible, as their main oxidation is through OH radicals during the daytime, as also noted by de Gouw et al. (2017). Furthermore, the other studies referred to in Table 1 for comparison have also reported emission ratios derived using only nighttime data.

Except for Lahore, where benzene levels were 10 times higher, benzene levels in Delhi were comparable to Beijing and about 3 times higher than those that have been reported from other megacities like São Paulo, London, Los Angeles, Paris, Mexico City, and New York. The annual-averaged national ambient air quality standard for benzene is 5 $\mu g\,m^{-3}$ in India, which is approximately 1.6 ppb at room temperature. Thus, the data suggest that sources in the investigated period (monsoon and post-monsoon season) would contribute to the violation of the annual-averaged values. Similarly, toluene

Table 1. Comparative summary of the average mixing ratio (ppb) and emission ratios of VOC / CO (ppb/ppm) of Delhi (in parentheses) with other megacities of Asia, Europe, and North America.

VOC	Delhi[a]	Lanzhou valley[b]	São Paulo[c]	London[d]	Los Angeles[e,f]	Paris[g,f]	Mexico City[h,k]	New York[e,l]	Beijing[i,m]	Lahore[j]
Benzene	2.02 (2.65)	0.54 (1.37)	0.67 (1.03)	0.31 (1.59)	0.48 (1.30)	0.38 (1.07)	0.80 (1.21)	0.74 (1.09)	1.79 (1.24)	28.20 (5.08)
Toluene	5.15 (7.03)	0.72 (1.41)	2.11 (3.1)	0.60 (3.09)	1.38 (3.18)	1.40 (12.30)	3.10 (4.20)	0.19 (3.79)	1.98 (2.41)	32.40 (6.67)
Sum of C8 aromatics	2.74 (4.20)	0.61 (1.42)	1.52 (2.15)	0.63 (3.69)	1.03 (2.45)	1.30 (4.75)	1.10 (4.30)	0.88 (1.11)	2.66 (2.15)	29.40 (6.04)

[a] This work (2022). [b] Zhou et al. (2019). [c] Brito et al. (2015). [d] Valach et al. (2014). [e] Baker et al. (2008). [f] Borbon et al. (2013). [g] Gros et al. (2011). [h] Garzón et al. (2015). [i] Yang et al. (2019). [j] Barletta et al. (2016). [k] Bon et al. (2011). [l] Warneke et al. (2007). [m] Wang et al. (2014).

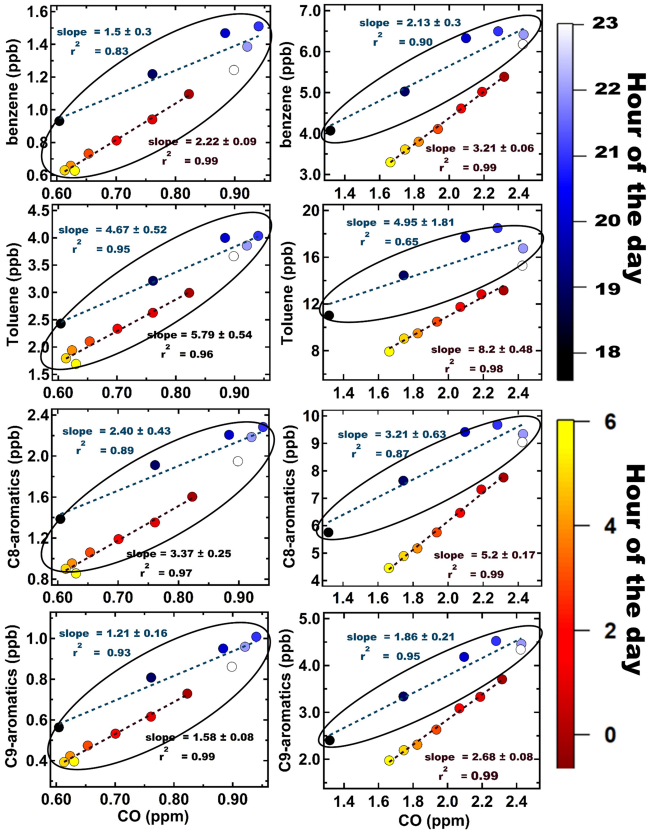

Figure 6. Emission ratios (VOC (ppb) / CO (ppm)) of benzene, toluene, C8 aromatics, and C9 aromatics for both monsoon (left panel) and post-monsoon (right panel) periods, respectively. The data points for each period are colour coded with the hour of the day (18:00 to 06:00 LT).

and the sum of C8 aromatic compounds (e.g. xylene and ethyl benzene isomers) were 6 to 10 times higher in Lahore compared to Delhi and more than twice as high relative to the aforementioned megacities, except for Beijing, where the sum of C8 aromatic compounds were comparable to Delhi. Overall, this indicates that Delhi has much higher levels of aromatic VOC pollution than many other megacities. When we peruse the emission ratios (ERs) that have been reported for these compounds in these other megacities (shown in parentheses in Table 1), barring few exceptions (e.g. Lahore and Paris), the ERs were generally much higher in Delhi, with an average value of 2.65, compared to cities like São Paulo (Brito et al., 2015), London (Valach et al., 2014), Los Angeles and Paris (Borbon et al., 2013), Mexico City (Bon et al., 2011), and several US cities (Baker et al., 2008). The ER of toluene was highest in Paris (12.3), followed by Delhi. Overall, the mixing ratios and ERs indicate that the influence of non-traffic sources (e.g. biomass burning and industries) is more significant in Delhi compared to many other megacities of the world. The companion paper on source apportionment based on this data set (Awasthi et al., 2024) will focus more on the quantitative contributions of the different sources.

4 Conclusion

This study has provided an unprecedented characterization of the VOC chemical composition of ambient air in Delhi for the clean monsoon and extremely polluted post-monsoon seasons. The total average mass concentration of the reactive carbon in the form of the 111 VOC species identified unambiguously was $\sim 260\,\mu g\,m^{-3}$ and more than 4 times higher during the polluted post-monsoon season, mainly due to the impact of large-scale open fires and reduced ventilation relative to the "cleaner" monsoon season. Of the 111, 42 were pure hydrocarbons (CH), 56 were oxygenated volatile organic compounds (OVOCs; CHO), 10 were nitrogen-containing compounds (NVOCs; CHON), 2 were chlorinated volatile organic compounds (ClVOCs), and 1, namely methanethiol, contained sulfur. The detection of new compounds that have previously not been observed in Delhi's air under both the clean and polluted periods, such as methanethiol, dichlorobenzenes, C6 amides, and C9 organic acids in the gas phase, was very surprising, considering that there have been several PTR-TOF-MS studies in Delhi before (Wang et al., 2020; Tripathi et al., 2022; Jain et al., 2022). Our data point to both industrial sources of the sulfur and chlorine compounds, photochemical sources of the C6 amides, and multiphase oxidation and chemical partitioning for the C9 organic acids. To our knowledge,

this is the first reported study worldwide to detect and observe only photochemically formed C6 amides in the gas phase. C6 amides are IVOCs, which can easily partition to the aerosol phase, depending on environmental conditions, and also act as a new source of reactive organic nitrogen in the atmospheric environment.

The monsoon season VOC abundances for major compounds were comparable to several other megacities of the world, showing that the baseline VOC levels for the city of Delhi due to year-round active sources, helped by favourable meteorological conditions for the removal of VOCs through ventilation and wet scavenging, can lead to comparable air quality, as observed in other megacities. The VOC levels during the polluted post-monsoon season when severe air pollution events occur, leading to shutdowns and curbs, on the other hand, were significantly (2–3 times) higher. Overall, for many important aromatic VOCs, the levels measured in Delhi were even higher (>5 times) than many other megacities of the world located in Europe and North America. Generally, these aromatic compounds in megacities are primarily due to traffic and industrial emission sources, and this source is of course common to Delhi and megacities in Europe and North America. In Delhi, the highest ambient mixing ratios of these aromatic compounds occurred in the post-monsoon season. This is the period when enhanced open biomass burning occurs due to the heating demand increase, owing to a dip in temperatures (Hakkim et al., 2019; Awasthi et al., 2024), and open-fire emissions due to the seasonal post-harvest paddy stubble biomass burning in which more than 1×10^7 t of biomass is burnt regionally (Kumar et al., 2021) within few weeks during mid-October to the end of November. This adds significantly to the atmospheric burden of these compounds compared to megacities in developed countries, where open biomass burning is better and more strictly regulated. Second, the meteorological conditions during the post-monsoon season due to a shallower boundary layer height and poor ventilation and lack of wet scavenging due to absence of rain also slow down atmospheric removal of these compounds compared to megacities in Europe, where it rains more frequently throughout the year compared to Delhi.

The presence of such a complex mixture of reactant VOCs adds to the air pollutant burden through secondary pollutant formation of aerosols. The reactive gaseous organics, which reached total averaged mass concentrations of $\sim 85\,\mu g\,m^{-3}$ (monsoon season) and $\sim 265\,\mu g\,m^{-3}$ (post-monsoon season), were found to rival the high mass concentrations of the main air pollutant in exceedance at this time, namely $PM_{2.5}$, during the extremely polluted periods (post-monsoon season average of $\sim 145\,\mu g\,m^{-3}$, which exceeds the 24 h national ambient air quality standard of $60\,\mu g\,m^{-3}$). The data of the time series of the $PM_{2.5}$ hourly data, along with acetonitrile (a biomass burning VOC tracer), measured at the same site is provided in Fig. S10. While the present study has quantified the molecules in the gas phase that are important for the air chemistry driving the high-pollution events in Delhi in unprecedented detail, the implications for secondary pollutant formation will require building up on this new strategic knowledge and further investigation. Moreover, the unique primary observations will yield a quantitative source apportionment of particulate matter and VOCs in a companion study (Awasthi et al., 2024) to enrich the scientific insights.

All previous VOC studies in the literature from a dynamically growing and changing megacity like Delhi were reported for periods before 2020 (pre-COVID-19) times, without the new enhanced volatility VOC quantification technology deployed for the first time in a complex ambient environment of a developing-world megacity like Delhi. These have resulted in unprecedented new information concerning the speciation, abundance, ambient variability, and emission characteristics of several rarely measured/reported VOCs. The significance of the new understanding concerning atmospheric composition and chemistry of highly polluted urban atmospheric environments gained from this study will no doubt be of global relevance, as they would aid atmospheric chemistry investigations in many megacities and polluted urban environments of the Global South that are in a similar development and growth trajectory to Delhi and experience extreme air pollution and air quality associated challenges but remain understudied.

Data availability. The primary VOC, CO, and ozone and meteorological data presented in this work can be downloaded from https://doi.org/10.17632/pb6xs2fzwc.1 (Sinha and Sinha, 2024). Boundary layer height data (m) for the period from 22 July to 26 November 2022 were retrieved from ERA5, which can be downloaded at https://doi.org/10.24381/cds.adbb2d47 (Hersbach et al., 2023).

Supplement. The supplement related to this article is available online at: https://doi.org/10.5194/acp-24-13129-2024-supplement.

Author contributions. SM: data curation, formal analysis, investigation, software, visualization, and writing (original draft preparation). VS: conceptualization, data curation, formal analysis, methodology, project administration, software, supervision, validation, and writing (review and editing). HH: data curation, formal analysis, investigation, and writing (review and editing). AA: data curation, formal analysis, and investigation. SDG: writing (review and editing). VKS: writing (review and editing). NN: resources. BS: conceptualization, data curation, supervision, and writing (review and editing). MNR: writing (review and editing).

Competing interests. The contact author has declared that none of the authors has any competing interests.

Acknowledgements. We acknowledge the financial support given by the Ministry of Earth Sciences (MOES), Government of India, to support the RASAGAM (Realtime Ambient Source Apportionment of Gases and Aerosol for Mitigation) project at IISER Mohali (grant no. MOES/16/06/2018-RDEAS; 22 June 2021). Sachin Mishra acknowledges IISER Mohali for the doctoral fellowship. Arpit Awasthi acknowledges the Ministry of Education, India, for the Prime Minister's Research Fellowship (PMRF) doctoral fellowship. We thank Rajamma Sukumaran Mahesh, Gopal Iyengar, Raghavan Krishnan (director, IITM Pune), Gowrishankar (director, IISER Mohali), Mohanty (DG, IMD), Muthalagu Ravichandran (secretary in the Ministry of Earth Science) for their encouragement and support. We thank the student members of the Atmospheric Chemistry and Emissions (ACE) research group and Aerosol Research Group (ARG) of IISER Mohali and IITM Pune, in particular Akash Vispute, Prasanna Lonkar, and the local scientists of IMD, for their logistics and moral support. The authors gratefully acknowledge the NASA/NOAA Suomi National Polar-orbiting Partnership (Suomi NPP) and NOAA-20 satellites VIIRS fire count data used in this publication. The authors gratefully acknowledge the NOAA Air Resources Laboratory (ARL) for the provision of the HYSPLIT transport and dispersion model used in this publication. We thank Campbell Scientific India Pvt Ltd, Ionicon Analytic GmbH, and Mars Bioanalytical Pvt. Ltd. for technical assistance rendered by them.

Financial support. This research has been funded by the Ministry of Earth Sciences (MoES), Government of India, to support the RASAGAM (Realtime Ambient Source Apportionment of Gases and Aerosol for Mitigation) project at IISER Mohali (grant no. MOES/16/06/2018-RDEAS; awarded on 22 June 2021).

Review statement. This paper was edited by Rebecca Garland and reviewed by two anonymous referees.

References

Acharja, P., Ali, K., Ghude, S. D., Sinha, V., Sinha, B., Kulkarni, R., Gultepe, I., and Rajeevan, M. N.: Enhanced secondary aerosol formation driven by excess ammonia during fog episodes in Delhi, India, Chemosphere 289, 133155, https://doi.org/10.1016/j.chemosphere.2021.133155, 2022.

Acharja, P., Ghude, S. D., Sinha, B., Barth, M., Govardhan, G., Kulkarni, R., Sinha, V., Kumar, R., Ali, K., Gultepe, I., Petit, J., and Rajeevan, M. N.: Thermodynamical framework for effective mitigation of high aerosol loading in the Indo-Gangetic Plain during winter, Sci. Rep., 13, 13667, https://doi.org/10.1038/s41598-023-40657-w, 2023.

Andreae, M. O.: Emission of trace gases and aerosols from biomass burning – an updated assessment, Atmos. Chem. Phys., 19, 8523–8546, https://doi.org/10.5194/acp-19-8523-2019, 2019.

Apel, E. C., Emmons, L. K., Karl, T., Flocke, F., Hills, A. J., Madronich, S., Lee-Taylor, J., Fried, A., Weibring, P., Walega, J., Richter, D., Tie, X., Mauldin, L., Campos, T., Weinheimer, A., Knapp, D., Sive, B., Kleinman, L., Springston, S., Zaveri, R., Ortega, J., Voss, P., Blake, D., Baker, A., Warneke, C., Welsh-Bon, D., de Gouw, J., Zheng, J., Zhang, R., Rudolph, J., Junkermann, W., and Riemer, D. D.: Chemical evolution of volatile organic compounds in the outflow of the Mexico City Metropolitan area, Atmos. Chem. Phys., 10, 2353–2375, https://doi.org/10.5194/acp-10-2353-2010, 2010.

ATSDR: Toxicological Profile for 1,4-Dichlorobenzene, Atlanta, GA, Agency for Toxic Substances and Disease Registry, U.S. Department of Health and Human Services, http://www.atsdr.cdc.gov/toxprofiles/tp10.pdf (last access: 15 February 2024), 2006.

Awasthi, A., Sinha, B., Hakkim, H., Mishra, S., Mummidivarapu, V., Singh, G., Ghude, S. D., Soni, V. K., Nigam, N., Sinha, V., and Rajeevan, M. N.: Biomass-burning sources control ambient particulate matter, but traffic and industrial sources control volatile organic compound (VOC) emissions and secondary-pollutant formation during extreme pollution events in Delhi, Atmos. Chem. Phys., 24, 10279–10304, https://doi.org/10.5194/acp-24-10279-2024, 2024.

Baker, A. K., Beyersdorf, A. J., Doezema, L. A., Katzenstein, A., Meinardi, S., Simpson, I. J., Blake, D. R., and Sherwood Rowland, F.: Measurements of nonmethane hydrocarbons in 28 United States cities, Atmos. Environ., 42, 170–182, https://doi.org/10.1016/j.atmosenv.2007.09.007, 2008.

Barletta, B., Simpson, I. J., Blake, N. J., Meinardi, S., Emmons, L. K., Aburizaiza, O. S., Siddique, A., Zeb, J., Yu, L. E., Khwaja, H. A., Farrukh, M. A., and Blake, D. R.: Characterization of carbon monoxide, methane and nonmethane hydrocarbons in emerging cities of Saudi Arabia and Pakistan and in Singapore, J. Atmos. Chem., 11, 2399–2421, https://doi.org/10.1007/s10874-016-9343-7, 2016.

Barnes, I., Solignac, G., Mellouki, A., and Becker, K. H.: Aspects of the atmospheric chemistry of amides, ChemPhysChem, 11, 3844–3857, https://doi.org/10.1002/cphc.201000374, 2010.

Bentley, R. and Chasteen, T. G.: Environmental VOSCs – formation and degradation of dimethyl sulfide, methanethiol and related materials, Chemosphere, 55, 291–317, https://doi.org/10.1016/j.chemosphere.2003.12.017, 2004.

Berresheim, H., Wine, P. H., and Davis, D. D.: Sulfur in the atmosphere, in: Composition, Chemistry, and Climate of the Atmosphere, edited by: Singh, H. B., Van Nostrand Reinhold, New York, 251–307, ISBN 0-442-01264-0, 1995.

Bikkina, S., Andersson, A., Kirillova, E. N., Holmstrand, H., Tiwari, S., Srivastava, A. K., Bisht, D. S., and Gustafsson, O.: Air quality in megacity Delhi affected by countryside biomass burning, Nat. Sustain., 2, 200–205, https://doi.org/10.1038/s41893-019-0219-0, 2019.

Bon, D. M., Ulbrich, I. M., de Gouw, J. A., Warneke, C., Kuster, W. C., Alexander, M. L., Baker, A., Beyersdorf, A. J., Blake, D., Fall, R., Jimenez, J. L., Herndon, S. C., Huey, L. G., Knighton, W. B., Ortega, J., Springston, S., and Vargas, O.: Measurements of volatile organic compounds at a suburban ground site (T1) in Mexico City during the MILAGRO 2006 campaign: measure-

ment comparison, emission ratios, and source attribution, Atmos. Chem. Phys., 11, 2399–2421, https://doi.org/10.5194/acp-11-2399-2011, 2011.

Borbon, A., Gilman, J. B., Kuster, W. C., Grand, N., Chevaillier, S., Colomb, A., Dolgorouky, C., Gros, V., Lopez, M., Sarda-Esteve, R., Holloway, J., Stutz, J., Petetin, H., McKeen, S., Beekmann, M., Warneke, C., Parrish, D. D., and de Gouw, J. A.: Emission ratios of anthropogenic volatile organic compounds in northern mid-latitude megacities: Observations versus emission inventories in Los Angeles and Paris, J. Geophys Res.-Atmos., 118, 2041–2057, https://doi.org/10.1002/jgrd.50059, 2013.

Borduas, N., da Silva, G., Murphy, J. G., and Abbatt, J. P.: Experimental and theoretical understanding of the gas phase oxidation of atmospheric amides with OH radicals: kinetics, products, and mechanisms, J. Phys. Chem. A, 119, 4298–4308, https://doi.org/10.1021/jp503759f, 2015.

Brito, J., Wurm, F., Yanez-Serrano, A. M., de Assuncao, J. V., Godoy, J. M., and Artaxo, P.: Vehicular Emission Ratios of VOCs in a Megacity Impacted by Extensive Ethanol Use: Results of Ambient Measurements in Sao Paulo, Brazil, Environ. Sci. Technol., 49, 11381–11387, https://doi.org/10.1021/acs.est.5b03281, 2015.

Bryant, D. J., Nelson, B. S., Swift, S. J., Budisulistiorini, S. H., Drysdale, W. S., Vaughan, A. R., Newland, M. J., Hopkins, J. R., Cash, J. M., Langford, B., Nemitz, E., Acton, W. J. F., Hewitt, C. N., Mandal, T., Gurjar, B. R., Shivani, Gadi, R., Lee, J. D., Rickard, A. R., and Hamilton, J. F.: Biogenic and anthropogenic sources of isoprene and monoterpenes and their secondary organic aerosol in Delhi, India, Atmos. Chem. Phys., 23, 61–83, https://doi.org/10.5194/acp-23-61-2023, 2023.

Bunkan, A. J. C., Mikoviny, T., Nielsen, C. J., Wisthaler, A., and Zhu, L.: Experimental and theoretical study of the OH-initiated photo-oxidation of formamide, J. Phys. Chem. A, 120, 1222–1230, https://doi.org/10.1021/acs.jpca.6b00032, 2016.

Cash, J. M., Langford, B., Di Marco, C., Mullinger, N. J., Allan, J., Reyes-Villegas, E., Joshi, R., Heal, M. R., Acton, W. J. F., Hewitt, C. N., Misztal, P. K., Drysdale, W., Mandal, T. K., Shivani, Gadi, R., Gurjar, B. R., and Nemitz, E.: Seasonal analysis of submicron aerosol in Old Delhi using high-resolution aerosol mass spectrometry: chemical characterisation, source apportionment and new marker identification, Atmos. Chem. Phys., 21, 10133–10158, https://doi.org/10.5194/acp-21-10133-2021, 2021.

Chandra, B. P. and Sinha, V.: Contribution of post-harvest agricultural paddy residue fires in the NW Indo-Gangetic Plain to ambient carcinogenic benzenoids, toxic isocyanic acid and carbon monoxide, Environ. Int., 88, 187–197, https://doi.org/10.1016/j.envint.2015.12.025, 2016.

Chandra, B. P., Sinha, V., Hakkim, H., Kumar, A., Pawar, H., Mishra, A. K., Sharma, G., Pallavi, Garg, S., Ghude, S. D., Chate, D. M., Pithani, P., Kulkarni, R., Jenamani, R. K., and Rajeevan, M.: Odd–even traffic rule implementation during winter 2016 in Delhi did not reduce traffic emissions of VOCs, carbon dioxide, methane and carbon monoxide, Curr. Sci. India, 114, 1318–1325, https://www.jstor.org/stable/26797338 (last access: 15 February 2024), 2018.

Chatterji, A.: Air Pollution in Delhi: Filling the Policy Gaps, ORF Occasional Paper No. 291, December 2020, Observer Research Foundation, https://www.orfonline.org/public/uploads/posts/pdf/20230723000625.pdf (last access: 10 February 2024), 2020.

Chen, T., Zhang, P., Chu, B., Ma, Q., Ge, Y., Liu, J., and He, H.: Secondary organic aerosol formation from mixed volatile organic compounds: Effect of RO_2 chemistry and precursor concentration, npj Climate and Atmospheric Science, 5, 95, https://doi.org/10.1038/s41612-022-00321-y, 2022.

Chin, J.-Y., Godwin, C., Jia, C., Robins, T., Lewis, T., Parker, E., Max, P., and Batterman, S.: Concentrations and risks of p-dichlorobenzene in indoor and outdoor air, Indoor Air, 23, 40–49, https://doi.org/10.1111/j.1600-0668.2012.00796.x, 2013.

Coggon, M. M., Stockwell, C. E., Claflin, M. S., Pfannerstill, E. Y., Xu, L., Gilman, J. B., Marcantonio, J., Cao, C., Bates, K., Gkatzelis, G. I., Lamplugh, A., Katz, E. F., Arata, C., Apel, E. C., Hornbrook, R. S., Piel, F., Majluf, F., Blake, D. R., Wisthaler, A., Canagaratna, M., Lerner, B. M., Goldstein, A. H., Mak, J. E., and Warneke, C.: Identifying and correcting interferences to PTR-ToF-MS measurements of isoprene and other urban volatile organic compounds, Atmos. Meas. Tech., 17, 801–825, https://doi.org/10.5194/amt-17-801-2024, 2024.

de Gouw, J. and Warneke, C.: Measurements of volatile organic compounds in the earth's atmosphere using proton-transfer-reaction mass spectrometry, Mass Spectrom. Rev., 26, 223–257, https://doi.org/10.1002/mas.20119, 2007.

de Gouw, J. A., Gilman, J. B., Kim, S.-W., Lerner, B. M., IsaacmanVanWertz, G., McDonald, B. C., Warneke, C., Kuster, W. C., Lefer, B. L., Griffith, S. M., Dusanter, S., Stevens, P. S., and Stutz, J.: Chemistry of Volatile Organic Compounds in the Los Angeles basin: Nighttime Removal of Alkenes and Determination of Emission Ratios, J. Geophys. Res.-Atmos., 122, 11843–11861, https://doi.org/10.1002/2017JD027459, 2017.

Dolgorouky, C., Gros, V., Sarda-Esteve, R., Sinha, V., Williams, J., Marchand, N., Sauvage, S., Poulain, L., Sciare, J., and Bonsang, B.: Total OH reactivity measurements in Paris during the 2010 MEGAPOLI winter campaign, Atmos. Chem. Phys., 12, 9593–9612, https://doi.org/10.5194/acp-12-9593-2012, 2012.

Durmusoglu, E., Taspinar, F., and Karademir, A.: Health risk assessment of BTEX emissions in the landfill environment, J. Hazard. Mater., 176, 870–877, https://doi.org/10.1016/j.jhazmat.2009.11.117, 2010.

Espenship, M. F., Silva, L. K., Smith, M. M., Capella, K. M., Reese, C. M., Rasio, J. P., Woodford, A. M., Geldner, N. B., Rey deCastro, B., and De Jesús, V. R.: Nitromethane exposure from tobacco smoke and diet in the US population: NHANES, 2007–2012, Environ. Sci. Technol., 53, 2134–2140, https://doi.org/10.1021/acs.est.8b05579, 2019.

Fang, M., Zheng, M., Wang, F., To, K. L., Jaafar, A. B., and Tong, S. L.: The solvent-extractable organic compounds in the Indonesia biomass burning aerosols–characterization studies, Atmos. Environ., 33, 783–795, https://doi.org/10.1016/S1352-2310(98)00210-6, 1999.

François, J. M.: Progress advances in the production of bio-sourced methionine and its hydroxyl analogues, Biotechnol. Adv., 69, 108259, https://doi.org/10.1016/j.biotechadv.2023.108259, 2023.

Gani, S., Bhandari, S., Patel, K., Seraj, S., Soni, P., Arub, Z., Habib, G., Hildebrandt Ruiz, L., and Apte, J. S.: Particle number concentrations and size distribution in a polluted megacity: the Delhi Aerosol Supersite study, Atmos. Chem. Phys., 20, 8533–8549, https://doi.org/10.5194/acp-20-8533-2020, 2020.

Garg, S., Chandra, B. P., Sinha, V., Sarda-Esteve, R., Gros, V., and Sinha, B.: Limitation of the use of the absorption angstrom exponent for source apportionment of equivalent black carbon: a case study from the North West Indo-Gangetic Plain, Environ. Sci. Technol., 50, 814–824, https://doi.org/10.1021/acs.est.5b03868, 2016.

Garzón, J. P., Huertas, J. I., Magaña, M., Huertas, M. E., Cárdenas, B., Watanabe, T., Maeda, T., Wakamatsu, S., and Blanco, S.: Volatile organic compounds in the atmosphere of Mexico City, Atmos. Environ., 119, 415–429, https://doi.org/10.1016/j.atmosenv.2015.08.014, 2015.

Graus, M., Müller, M., and Hansel, A.: High resolution PTR-TOF: quantification and formula confirmation of VOC in real time, J. Am. Soc. Mass Spectr., 21, 1037–1044, https://doi.org/10.1016/j.jasms.2010.02.006, 2011.

Gros, V., Gaimoz, C., Herrmann, F., Custer, T., Williams, J., Bonsang, B., Sauvage, S., Locoge, N., d'Argouges, O., Sarda-Esteve, R., and Sciare, J.: Volatile organic compounds sources in Paris in spring 2007. Part I: qualitative analysis, Environ. Chem., 8, 74–90, 2011.

Guttikunda, S. K., Dammalapati,, S. K., Pradhan, G., Krishna, B., Jethva, H. T., and Jawahar, P.: What Is Polluting Delhi's Air? A Review from 1990 to 2022, Sustainability, 15, 4209, https://doi.org/10.3390/su15054209, 2023.

Hakkim, H., Sinha, V., Chandra, B. P., Kumar, A., Mishra, A. K., Sinha, B., Sharma, G., Pawar, H., Sohpaul, B., Ghude, S. D., Pithani, P., Kulkarni, R., Jenamani, R. K., and Rajeevan, M.: Volatile organic compound measurements point to fog-induced biomass burning feedback to air quality in the megacity of Delhi, Sci. Total Environ., 689, 295–304, https://doi.org/10.1016/j.scitotenv.2019.06.438, 2019.

Hakkim, H., Kumar, A., Annadate, S., Sinha, B., and Sinha, V.: RTEII: A new high-resolution ($0.1^\circ \times 0.1^\circ$) road transport emission inventory for India of 74 speciated NMVOCs, CO, NO_x, NH_3, CH_4, CO_2, $PM_{2.5}$ reveals massive overestimation of NO_x and CO and missing nitromethane emissions by existing inventories, Atmos. Environ. X, 11, 100118, https://doi.org/10.1016/j.aeaoa.2021.100118, 2021.

Hatakeyama, S. and Akimoto, H.: Reactions of hydroxyl radicals with methanethiol, dimethyl sulfide, and dimethyl disulfide in air, J. Phy. Chem., 87, 2387–2395, 1983.

Hatch, L. E., Yokelson, R. J., Stockwell, C. E., Veres, P. R., Simpson, I. J., Blake, D. R., Orlando, J. J., and Barsanti, K. C.: Multi-instrument comparison and compilation of non-methane organic gas emissions from biomass burning and implications for smoke-derived secondary organic aerosol precursors, Atmos. Chem. Phys., 17, 1471–1489, https://doi.org/10.5194/acp-17-1471-2017, 2017.

Hearn, C. H., Turcu, E., and Joens, J. A.: The near U.V. absorption spectra of dimethyl sulfide, diethyl sulfide and dimethyl disulfide at $T = 300$ K, Atmos. Environ., 24A, 1939–1944, 1990.

Hersbach, H., Bell, B., Berrisford, P., Biavati, G., Horányi, A., Muñoz Sabater, J., Nicolas, J., Peubey, C., Radu, R., Rozum, I., Schepers, D., Simmons, A., Soci, C., Dee, D., and Thépaut, J.-N.: ERA5 hourly data on single levels from 1940 to present, Copernicus Climate Change Service (C3S) Climate Data Store (CDS) [data set], https://doi.org/10.24381/cds.adbb2d47, 2023.

Ho, S. S. H., Yu, J. Z., Chu, K. W., and Yeung, L. L.: Carbonyl Emissions from Commercial Cooking Sources in Hong Kong, J. Air Waste Manage. Assoc., 56, 1091–1098, https://doi.org/10.1080/10473289.2006.10464532, 2006.

Holzinger, R., Warneke, C., Hansel, A., Jordan, A., Lindinger, W., Scharffe, D. H., Schade, G., and Crutzen, P. J.: Biomass burn ing as a source of formaldehyde, acetaldehyde, methanol, ace tone, acetonitrile, and hydrogen cyanide, Geophys. Res. Lett., 26, 1161–1164, https://doi.org/10.1029/1999gl900156, 1999.

Hu, Y., Ma, J., Zhu, M., Zhao, Y., Peng, S., and Zhu, C.: Photochemical oxidation of o-dichlorobenzene in aqueous solution by hydroxyl radicals from nitrous acid, J. Photoch. Photobio. A, 420, 113503, https://doi.org/10.1016/j.jphotochem.2021.113503, 2021.

Jain, V., Tripathi, S. N., Tripathi, N., Sahu, L. K., Gaddamidi, S., Shukla, A. K., Bhattu, D., and Ganguly, D.: Seasonal variability and source apportionment of non-methane VOCs using PTR-TOF-MS measurements in Delhi, India, Atmos. Environ. 283, 119163, https://doi.org/10.1016/j.atmosenv.2022.119163, 2022.

Jordan, A., Haidacher, S., Hanel, G., Hartungen, E., Märk, L., Seehauser, H., Schottkowsky, R., Sulzer, P., and Märk, T. D.: A high resolution and high sensitivity proton-transfer-reaction time-offlight mass spectrometer (PTR-TOF-MS), Int. J. Mass Spectrom., 286, 122–128, https://doi.org/10.1016/j.ijms.2009.07.005, 2009.

Kadota, H., and Ishida, Y.: Production of volatile sulfur compounds by microorganisms, Annu. Rev. Microbiol., 26, 127–138, https://doi.org/10.1146/annurev.mi.26.100172.001015, 1972.

Kawamura, K., Okuzawa, K., Aggarwal, S. G., Irie, H., Kanaya, Y., and Wang, Z.: Determination of gaseous and particulate carbonyls (glycolaldehyde, hydroxyacetone, glyoxal, methylglyoxal, nonanal and decanal) in the atmosphere at Mt. Tai, Atmos. Chem. Phys., 13, 5369–5380, https://doi.org/10.5194/acp-13-5369-2013, 2013.

Keywood, M., Paton-Walsh, C., Lawrence, M. G., George, C., Formenti, P., Schofield, R., Cleugh, H., Borgford-Parnell, N., and Capon, A.: Atmospheric goals for sustainable development, Science, 379, 246–247, https://doi.org/10.1126/science.adg2495, 2023.

Kim, K.: Emissions of reduced sulfur compounds (RSC) as a landfill gas (LFG): a comparative study of young and old landfill facilities, Atmos. Environ., 40, 6567–6578, https://doi.org/10.1016/j.atmosenv.2006.05.063, 2006.

Komae, S., Sekiguchi, K., Suzuki, M., Nakayama, R., Namiki, N., and Kagi, N.: Secondary organic aerosol formation from p-dichlorobenzene under indoor environmental conditions, Build. Environ,, 174, 106758, https://doi.org/10.1016/j.buildenv.2020.106758, 2020.

Koss, A. R., Sekimoto, K., Gilman, J. B., Selimovic, V., Coggon, M. M., Zarzana, K. J., Yuan, B., Lerner, B. M., Brown, S. S., Jimenez, J. L., Krechmer, J., Roberts, J. M., Warneke, C., Yokelson, R. J., and de Gouw, J.: Non-methane organic gas emissions from biomass burning: identification, quantification, and emission factors from PTR-ToF during the FIREX 2016 laboratory experiment, Atmos. Chem. Phys., 18, 3299–3319, https://doi.org/10.5194/acp-18-3299-2018, 2018.

Kulkarni, S. H., Ghude, S. D., Jena, C., Karumuri, R. K., Sinha, B., Sinha, V., Kumar, R., Soni, V. K., and Khare, M.: How much does large-scale crop residue burning affect the air quality in Delhi?, Environ. Sci. Technol., 54, 4790–4799, https://doi.org/10.1021/acs.est.0c00329, 2020.

Kumar, A., Sinha, V., Shabin, M., Hakkim, H., Bonsang, B., and Gros, V.: Non-methane hydrocarbon (NMHC) fingerprints of major urban and agricultural emission sources for use in source apportionment studies, Atmos. Chem. Phys., 20, 12133–12152, https://doi.org/10.5194/acp-20-12133-2020, 2020.

Kumar, A., Hakkim, H., Sinha, B., and Sinha, V.: Gridded 1 km × 1 km emission inventory for paddy stubble burning emissions over north-west India constrained by measured emission factors of 77 VOCs and district-wise crop yield data, Sci. Total Environ., 789, 148064, https://doi.org/10.1016/j.scitotenv.2021.148064, 2021.

Kumar, V., Sarkar, C., and Sinha, V.: Influence of post-harvest crop residue fires on surface ozone mixing ratios in the NW IGP analyzed using 2 years of continuous in situ trace gas measurements, J. Geophys. Res.-Atmos., 121, 3619–3633, https://doi.org/10.1002/2015JD024308, 2016.

Kumar, V., Chandra, B. P., and Sinha, V.: Large unexplained suite of chemically reactive compounds present in ambient air due to biomass fires, Sci. Rep., 8, 626, https://doi.org/10.1038/s41598-017-19139-3, 2018.

Langford, B., Nemitz, E., House, E., Phillips, G. J., Famulari, D., Davison, B., Hopkins, J. R., Lewis, A. C., and Hewitt, C. N.: Fluxes and concentrations of volatile organic compounds above central London, UK, Atmos. Chem. Phys., 10, 627–645, https://doi.org/10.5194/acp-10-627-2010, 2010.

Lelieveld, J., Evans, J. S., Fnais, M., Giannadaki, D., and Pozzer, A.: The contribution of outdoor air pollution sources to premature mortality on a global scale, Nature 525, 367–371, https://doi.org/10.1038/nature15371, 2015.

Li, K., Li, J., Tong, S., Wang, W., Huang, R.-J., and Ge, M.: Characteristics of wintertime VOCs in suburban and urban Beijing: concentrations, emission ratios, and festival effects, Atmos. Chem. Phys., 19, 8021–8036, https://doi.org/10.5194/acp-19-8021-2019, 2019.

Li, Y., Pöschl, U., and Shiraiwa, M.: Molecular corridors and parameterizations of volatility in the chemical evolution of organic aerosols, Atmos. Chem. Phys., 16, 3327–3344, https://doi.org/10.5194/acp-16-3327-2016, 2016.

Lin, P., Liu, J., Shilling, J. E., Kathmann, S. M., Laskin J., and Laskin, A.: Molecular characterization of brown carbon (BrC) chromophores in secondary organic aerosol generated from photo-oxidation of toluene, Phys. Chem. Chem. Phys., 17, 23312–23325, https://doi.org/10.1039/c5cp02563j, 2015.

Lin, P., Bluvshtein, N., Rudich, Y., Nizkorodov, S. A., Laskin, J., and Laskin, A.: Molecular Chemistry of Atmospheric Brown Carbon Inferred from a Nationwide Biomass Burning Event, Environ. Sci. Technol., 51, 11561–11570, https://doi.org/10.1021/acs.est.7b02276, 2017.

Mackay, D., Shiu, W. Y., and Ma, K. C.: Illustrated handbook of physical-chemical properties of environmental fate for organic chemicals, Vol. 5, CRC press, 832 pp., ISBN 978-1-56670-255-3, 1997.

McDonald, B. C., de Gouw, J. A., Gilman, J. B., Jathar, S. H., Akherati, A., Cappa, C. D., Jimenez, J. L., Lee-Taylor, J., Hayes, P. L., McKeen, S. A., Cui, Y. Y., Kim, S. W., Gentner, D. R., Isaacman-VanWertz, G., Goldstein, A. H., Harley, R. A., Frost, G. J., Roberts, J. M., Ryerson, T. B., and Trainer, M.: Volatile chemical products emerging as largest petrochemical source of urban organic emissions, Science, 359, 760–764, https://doi.org/10.1126/science.aaq0524, 2018.

Millet, D. B., Guenther, A., Siegel, D. A., Nelson, N. B., Singh, H. B., de Gouw, J. A., Warneke, C., Williams, J., Eerdekens, G., Sinha, V., Karl, T., Flocke, F., Apel, E., Riemer, D. D., Palmer, P. I., and Barkley, M.: Global atmospheric budget of acetaldehyde: 3-D model analysis and constraints from in-situ and satellite observations, Atmos. Chem. Phys., 10, 3405–3425, https://doi.org/10.5194/acp-10-3405-2010, 2010.

Mishra, A. K. and Sinha, V.: Emission drivers and variability of ambient isoprene, formaldehyde and acetaldehyde in north-west India during monsoon season, Environ. Pollut., 267, 115538, https://doi.org/10.1016/j.envpol.2020.115538, 2020.

Müller, M., Mikoviny, T., Feil, S., Haidacher, S., Hanel, G., Hartungen, E., Jordan, A., Märk, L., Mutschlechner, P., Schottkowsky, R., Sulzer, P., Crawford, J. H., and Wisthaler, A.: A compact PTR-ToF-MS instrument for airborne measurements of volatile organic compounds at high spatiotemporal resolution, Atmos. Meas. Tech., 7, 3763–3772, https://doi.org/10.5194/amt-7-3763-2014, 2014.

Nault, B. A., Jo, D. S., McDonald, B. C., Campuzano-Jost, P., Day, D. A., Hu, W., Schroder, J. C., Allan, J., Blake, D. R., Canagaratna, M. R., Coe, H., Coggon, M. M., DeCarlo, P. F., Diskin, G. S., Dunmore, R., Flocke, F., Fried, A., Gilman, J. B., Gkatzelis, G., Hamilton, J. F., Hanisco, T. F., Hayes, P. L., Henze, D. K., Hodzic, A., Hopkins, J., Hu, M., Huey, L. G., Jobson, B. T., Kuster, W. C., Lewis, A., Li, M., Liao, J., Nawaz, M. O., Pollack, I. B., Peischl, J., Rappenglück, B., Reeves, C. E., Richter, D., Roberts, J. M., Ryerson, T. B., Shao, M., Sommers, J. M., Walega, J., Warneke, C., Weibring, P., Wolfe, G. M., Young, D. E., Yuan, B., Zhang, Q., de Gouw, J. A., and Jimenez, J. L.: Secondary organic aerosols from anthropogenic volatile organic compounds contribute substantially to air pollution mortality, Atmos. Chem. Phys., 21, 11201–11224, https://doi.org/10.5194/acp-21-11201-2021, 2021.

Nelson, B. S., Stewart, G. J., Drysdale, W. S., Newland, M. J., Vaughan, A. R., Dunmore, R. E., Edwards, P. M., Lewis, A. C., Hamilton, J. F., Acton, W. J., Hewitt, C. N., Crilley, L. R., Alam, M. S., Şahin, Ü. A., Beddows, D. C. S., Bloss, W. J., Slater, E., Whalley, L. K., Heard, D. E., Cash, J. M., Langford, B., Nemitz, E., Sommariva, R., Cox, S., Shivani, Gadi, R., Gurjar, B. R., Hopkins, J. R., Rickard, A. R., and Lee, J. D.: In situ ozone production is highly sensitive to volatile organic compounds in Delhi, India, Atmos. Chem. Phys., 21, 13609–13630, https://doi.org/10.5194/acp-21-13609-2021, 2021.

Nielsen, C. J., Herrmann, H., and Weller, C.: Atmospheric chemistry and environmental impact of the use of amines in carbon capture and storage (CCS), Chem. Soc. Rev., 41, 6684–6704, https://doi.org/10.1039/C2CS35059A, 2012.

Nunes, L. S., Tavares, T. M., Dippel, J., and Jaeschke, W.: Measurements of Atmospheric Concentrations of Reduced Sulphur Compounds in the All Saints Bay Area in Bahia, Brazil, J. Atmos. Chem., 50, 79–100, https://doi.org/10.1007/s10874-005-3123-0, 2005.

Oros, D. R., bin Abas, M. R., Omar, N. Y. M., Rahman, N. A., and Simoneit, B. R.: Identification and emission factors of molecular tracers in organic aerosols from biomass burning: Part 3. Grasses, Appl. Geochem., 21, 919–940, https://doi.org/10.1016/j.apgeochem.2006.01.008, 2006.

Pagonis, D., Sekimoto, K., and de Gouw, J.: A library of proton-transfer reactions of H_3O^+ ions used for trace gas detection, J. Am. Soc. Mass Spectr., 30, 1330–1335, https://doi.org/10.1007/s13361-019-02209-3, 2019.

Pawar, H., Garg, S., Kumar, V., Sachan, H., Arya, R., Sarkar, C., Chandra, B. P., and Sinha, B.: Quantifying the contribution of long-range transport to particulate matter (PM) mass loadings at a suburban site in the north-western Indo-Gangetic Plain (NW-IGP), Atmos. Chem. Phys., 15, 9501–9520, https://doi.org/10.5194/acp-15-9501-2015, 2015.

Pawar, P. V., Ghude, S. D., Govardhan, G., Acharja, P., Kulkarni, R., Kumar, R., Sinha, B., Sinha, V., Jena, C., Gunwani, P., Adhya, T. K., Nemitz, E., and Sutton, M. A.: Chloride (HCl / Cl^-) dominates inorganic aerosol formation from ammonia in the Indo-Gangetic Plain during winter: modeling and comparison with observations, Atmos. Chem. Phys., 23, 41–59, https://doi.org/10.5194/acp-23-41-2023, 2023.

Piel, F., Müller, M., Winkler, K., Skytte af Sätra, J., and Wisthaler, A.: Introducing the extended volatility range proton-transfer-reaction mass spectrometer (EVR PTR-MS), Atmos. Meas. Tech., 14, 1355–1363, https://doi.org/10.5194/amt-14-1355-2021, 2021.

Reed, N. W., Browne, E. C., and Tolbert, M. A.: Impact of hydrogen sulfide on photochemical haze formation in methane/nitrogen atmospheres, ACS Earth Space Chem., 4, 897–904, https://doi.org/10.1021/acsearthspacechem.0c00086, 2020.

Reinecke, T., Leiminger, M., Klinger, A., and Müller, M.: Direct detection of polycyclic aromatic hydrocarbons on a molecular composition level in summertime ambient aerosol via proton transfer reaction mass spectrometry, Aerosol Research, 2, 225–233, https://doi.org/10.5194/ar-2-225-2024, 2024.

Roberts, J. M., Veres, P. R., Cochran, A. K., Warneke, C., Burling, I. R., Yokelson, R. J., Lerner, B., Gilman, J. B., Kuster, W. C., Fall, R., and de Gouw, J.: Isocyanic acid in the atmosphere and its possible link to smoke-related health effects, P. Natl. Acad. Sci. USA, 108, 8966–8971, https://doi.org/10.1073/pnas.1103352108, 2011.

Salvador, C. M., Chou, C. C. K., Ho, T. T., Ku, I. T., Tsai, C. Y., Tsao, T. M., Tsai, M. J., and Su, T. C.: Extensive urban air pollution footprint evidenced by submicron organic aerosols molecular composition, npj Climate and Atmospheric Science, 5, 96, https://doi.org/10.1038/s41612-022-00314-x, 2022.

Sarkar, C., Sinha, V., Kumar, V., Rupakheti, M., Panday, A., Mahata, K. S., Rupakheti, D., Kathayat, B., and Lawrence, M. G.: Overview of VOC emissions and chemistry from PTR-TOF-MS measurements during the SusKat-ABC campaign: high acetaldehyde, isoprene and isocyanic acid in wintertime air of the Kathmandu Valley, Atmos. Chem. Phys., 16, 3979–4003, https://doi.org/10.5194/acp-16-3979-2016, 2016.

Shabin, M., Khatarkar, P., Hakkim, H., Awasthi, A., Mishra, S., and Sinha, V.: Monsoon and post-monsoon measurements of 53 non-methane hydrocarbons (NMHCs) in megacity Delhi and Mohali reveal similar NMHC composition across seasons, Urban Climate, 55, 101983, https://doi.org/10.1016/j.uclim.2024.101983, 2024.

Sharma, S. K. and Mandal, T. K.: Elemental composition and sources of fine particulate matter ($PM_{2.5}$) in Delhi, India, B. Environ. Contam. Tox., 110, 60, https://doi.org/10.1007/s00128-023-03707-7, 2023.

Singh, D. P., Gadi, R., and Mandal, T. K.: Characterization of particulate-bound polycyclic aromatic hydrocarbons and trace metals composition of urban air in Delhi, India, Atmos. Environ., 45, 7653–7663, https://doi.org/10.1016/j.atmosenv.2011.02.058, 2011.

Singh, R., Sinha, B., Hakkim, H., and Sinha, V.: Source apportionment of volatile organic compounds during paddy-residue burning season in north-west India reveals large pool of photochemically formed air toxics, Environ. Pollut., 338, 122656, https://doi.org/10.1016/j.envpol.2023.122656, 2023.

Sinha, V. and Sinha, B.: VOCdataset_2022_MPMDelhi, Mendeley Data, V1 [data set], https://doi.org/10.17632/pb6xs2fzwc.1, 2024.

Sinha, V., Kumar, V., and Sarkar, C.: Chemical composition of premonsoon air in the Indo-Gangetic Plain measured using a new air quality facility and PTR-MS: high surface ozone and strong influence of biomass burning, Atmos. Chem. Phys., 14, 5921–5941, https://doi.org/10.5194/acp-14-5921-2014, 2014.

Stark, H., Yatavelli, R. L. N., Thompson, S. L., Kimmel, J. R., Cubison, M. J., Chhabra, P. S., Canagaratna, M. R., Jayne, J. T., Worsnop, D. R., and Jimenez, J. L.: Methods to extract molecular and bulk chemical information from series of complex mass spectra with limited mass resolution, Int. J. Mass Spectrom., 389, 26–38, https://doi.org/10.1016/j.ijms.2015.08.011, 2015.

Stockwell, C. E., Veres, P. R., Williams, J., and Yokelson, R. J.: Characterization of biomass burning emissions from cooking fires, peat, crop residue, and other fuels with high-resolution proton-transfer-reaction time-of-flight mass spectrometry, Atmos. Chem. Phys., 15, 845–865, https://doi.org/10.5194/acp-15-845-2015, 2015.

Toda, K., Obata, T., Obokin, V. A., Potemkin, V. L., Hirota, K., Takeuchi, M., Arita, S., Khodzher, T. V., and Grachev, M. A.: Atmospheric methanethiol emitted from a pulp and paper plant on the shore of Lake Baikal, Atmos. Environ., 44, 2427–2433, https://doi.org/10.1016/j.atmosenv.2010.03.037, 2010.

Tripathi, N., Sahu, L. K., Wang, L., Vats, P., Soni, M., Kumar, P., Satish, R. V., Bhattu, D., Sahu, R., Patel, K., Rai, P., Kumar, V., Rastogi, N., Ojha, N., Tiwari, S., Ganguly, D., Slowik, J., Prévôt, A. S. H., and Tripathi, S. N.: Characteristics of VOC Composition at Urban and Suburban Sites of New Delhi, India in Winter, J. Geophys. Res.-Atmos., 127, e2021JD035342, https://doi.org/10.1029/2021JD035342, 2022.

Valach, A. C., Langford, B., Nemitz, E., MacKenzie, A. R., and Hewitt, C. N.: Concentrations of selected volatile organic compounds at kerbside and background sites in central London, Atmos. Environ., 95, 456–467, https://doi.org/10.1016/j.atmosenv.2014.06.052, 2014.

von Hartungen, E., Wisthaler, A., Mikoviny, T., Jaksch, D., Boscaini, E., Dunphy, P. J., and Märk, T. D.: Proton-transfer reaction mass spectrometry (PTR-MS) of carboxylic acids. Determination of Henry's law constants and axillary odour investigations, Int. J. Mass Spectrom., 239, 243–248, https://doi.org/10.1016/j.ijms.2004.09.009, 2004.

Wang, M., Shao, M., Chen, W., Yuan, B., Lu, S., Zhang, Q., Zeng, L., and Wang, Q.: A temporally and spatially resolved validation of emission inventories by measurements of ambient volatile organic compounds in Beijing, China, Atmos. Chem. Phys., 14, 5871–5891, https://doi.org/10.5194/acp-14-5871-2014, 2014.

Wang, L., Slowik, J. G., Tripathi, N., Bhattu, D., Rai, P., Kumar, V., Vats, P., Satish, R., Baltensperger, U., Ganguly, D., Rastogi, N., Sahu, L. K., Tripathi, S. N., and Prévôt, A. S. H.: Source characterization of volatile organic compounds measured by proton-transfer-reaction time-of-flight mass spectrometers in Delhi, India, Atmos. Chem. Phys., 20, 9753–9770, https://doi.org/10.5194/acp-20-9753-2020, 2020.

Warneke, C., Holzinger, R., Hansel, A., Jordan, A., Lindinger, W., Poschl, U., Williams, J., Hoor, P., Fischer, H., Crutzen, P. J., Scheeren, H. A., and Lelieveld, J.: Isoprene and its oxidation products methyl vinyl ketone, methacrolein, and isoprene related peroxides measured online over the tropical rain forest of Surinam in March 1998, J. Atmos. Chem., 38, 167–185, https://doi.org/10.1023/A:1006326802432, 2001.

Warneke, C., McKeen, S. A., de Gouw, J. A., Goldan, P. D., Kuster, W. C., Holloway, J. S., Williams, E. J., Lerner, B. M., Parrish, D. D., Trainer, M., Fehsenfeld, F. C., Kato, S., Atlas, E. L., Baker, A., and Blake, D. R.: Determination of urban volatile organic compound emission ratios and comparison with an emissions database, J. Geophys. Res., 112, D10S47, https://doi.org/10.1029/2006JD007930, 2007.

Weng, M., Zhu, L., Yang, K., and Chen, S.: Levels and health risks of carbonyl compounds in selected public places in Hangzhou, China, J. Hazard. Mater., 164, 700–706, https://doi.org/10.1016/j.jhazmat.2008.08.094, 2009.

WHO: Guidelines for Indoor Air Quality: Selected Pollutants, edited by: Theakston, F., World Health Organization: WHO Regional Office for Europe, Copenhagen, Denmark, 1–454, ISBN 978-92-89002-14-1, 2010.

WHO: Exposure to benzene: a major public health concern, WHO, https://www.who.int/publications/i/item/WHO-CED-PHE-EPE-19.4.2 (last access: 19 January 2024), 2019.

Wine, P. H., Kreutter, N. M., Gump, C. A., and Ravishankara, A. R.: Kinetics of hydroxyl radical reactions with the atmospheric sulfur compounds hydrogen sulfide, methanethiol, ethanethiol, and dimethyl disulfide, J. Phys. Chem., 85, 2660–2665, 1981.

Yáñez-Serrano, A. M., Filella, I., LLusià, J., Gargallo-Garriga, A., Granda, V., Bourtsoukidis, E., Williams, J., Seco, R., Cappellin, L., Werner, C., de Gouw, J., and Peñuelas, J.: GLOVOCS – Master compound assignment guide for proton transfer reaction mass spectrometry users, Atmos. Environ., 244, 117929, https://doi.org/10.1016/J.ATMOSENV.2020.117929, 2021.

Yang, Y., Ji, D., Sun, J., Wang, Y., Yao, D., Zhao, S., Yu, X., Zeng, L., Zhang, R., Zhang, H., Wang, Y., and Wang, Y.: Ambient volatile organic compounds in a suburban site between Beijing and Tianjin: Concentration levels, source apportionment and health risk assessment, Sci. Total Environ., 695, 133889, https://doi.org/10.1016/j.scitotenv.2019.133889, 2019.

Yao, L., Wang, M.-Y., Wang, X.-K., Liu, Y.-J., Chen, H.-F., Zheng, J., Nie, W., Ding, A.-J., Geng, F.-H., Wang, D.-F., Chen, J.-M., Worsnop, D. R., and Wang, L.: Detection of atmospheric gaseous amines and amides by a high-resolution time-of-flight chemical ionization mass spectrometer with protonated ethanol reagent ions, Atmos. Chem. Phys., 16, 14527–14543, https://doi.org/10.5194/acp-16-14527-2016, 2016.

Yoshino, A., Nakashima, Y., Miyazaki, K., Kato, S., Suthawaree, J., Shimo, N., Matsunaga, S., Chatani, S., Apel, E., Greenberg, J., Guenther, A., Ueno, H., Sasaki, H., Hoshi, J. Y., Yokota, H., Ishii, K., and Kajii, Y.: Air quality diagnosis from comprehensive observations of total OH reactivity and reactive trace species in urban central Tokyo, Atmos. Environ., 49, 51–59, https://doi.org/10.1016/j.atmosenv.2011.12.029, 2012.

Yuan, B., Koss, A. R., Warneke, C., Coggon, M., Sekimoto, K., and de Gouw, J.: Proton-Transfer Reaction Mass Spectrometry: Applications in Atmospheric Sciences, Chem. Rev., 117, 13187–13229, https://doi.org/10.1021/acs.chemrev.7b00325, 2017.

Zhou, X., Li, Z., Zhang, T., Wang, F., Wang, F., Tao, Y., Zhang, X., Wang, F., and Huang, J.: Volatile organic compounds in a typical petrochemical industrialized valley city of northwest China based on high-resolution PTR-MS measurements: Characterization, sources and chemical effects, Sci. Total Environ., 671, 883–896, https://doi.org/10.1016/j.scitotenv.2019.03.283, 2019.